JOC The Journal of Organic Chemistry

Article

Development of a Convergent Large-Scale Synthesis for Venetoclax, a First-in-Class BCL-2 Selective Inhibitor

Yi-Yin Ku, Vincent S Chan, Alan Christesen, Timothy Grieme, Mathew Mulhern, Yu-Ming Pu, and Michael D. Wendt

J. Org. Chem., **Just Accepted Manuscript** • DOI: 10.1021/acs.joc.8b02750 • Publication Date (Web): 07 Jan 2019

Just Accepted

ACS Publications

is published by the American Chemical Society. 1155 Sixteenth Street N.W., Washington, DC 20036

Development of a Convergent Large-Scale Synthesis for Venetoclax, a First-in-Class BCL-2 Selective Inhibitor

Yi-Yin Ku,[1] Vincent S. Chan,[3] Alan Christesen,[1] Timothy Grieme,[1] Mathew Mulhern,[1] Yu-Ming Pu[1] and Michael D Wendt[2]*

1 Process Chemistry, Pharmaceutical Research and Development, Abbvie.

2. Medicinal Chemistry, Pharmaceutical Research and Development, Abbvie

3. Current contact information: vchan@seagen.com

1 North Waukegan Road

North Chicago, IL 60064, United States

Venclexta™, Venetoclax, BCL-2 Inhibitor, ABT-199, Manufacture Process

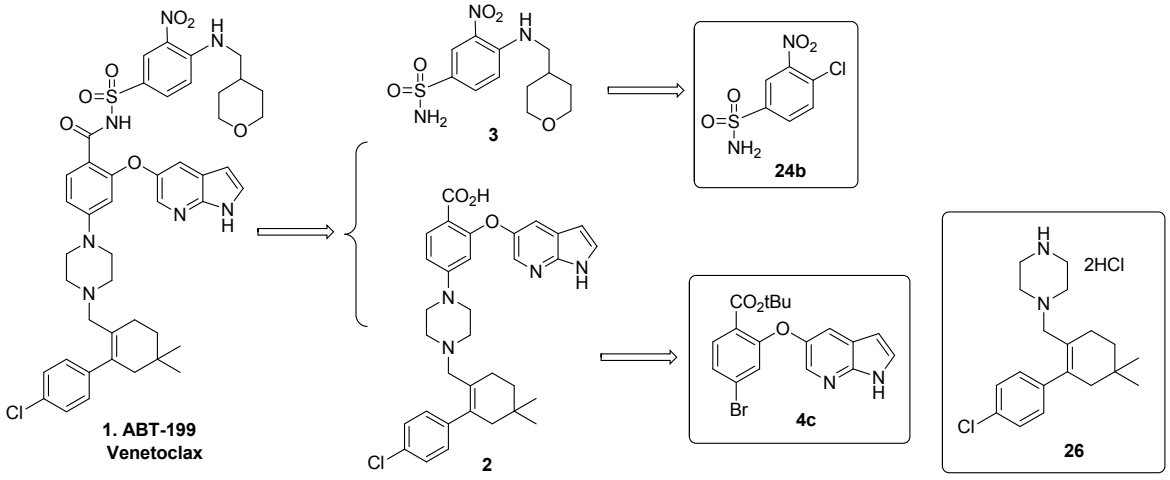

ABSTRACT: The process development of a new synthetic route leading to an efficient and robust synthetic process for Venetoclax (**1**: the active pharmaceutical ingredient (API) in Venclexta™) is described. The redesigned synthesis features a Buchwald-Hartwig amination to construct the core ester **23c** in a convergent fashion by connecting two key building blocks (**4c** and **26**), which is then followed by a uniquely effective saponification reaction of **23c** using anhydrous hydroxide generated *in-situ* to obtain **2**. Finally, the coupling of the penultimate core acid **2** with sulfonamide **3** furnishes drug substance **1** with consistently high quality. The challenges and solutions for the key Pd-catalyzed C-N cross-coupling will also be discussed in detail. The improved synthesis overcomes many of the initial scale-up challenges and was accomplished in 46% overall yield from 3,3-dimethyldicyclohexanone **6**, more than doubling the overall yield of the first generation route. The new process was successfully implemented for producing large quantities of **1** with >99% area purity.

1. INTRODUCTION

Venetoclax **1** (Figure 1), [1-4] the active pharmaceutical ingredient (API) of Venclexta™, obtained accelerated approval from the U.S. Food and Drug Administration (FDA)) in April 2016 [1] as the first small molecule BCL-2 selective inhibitor for the treatment of relapsed/refractory chronic lymphocytic leukemia (CLL) patients with the 17p deletion genetic mutation.Venclexta is currently being investigated in a number of other indications. Recently, it obtained FDA approval under priority review as a combination therapy with rituximab for treating patients with CLL or small lymphocytic lymphoma (SLL) with or without the 17p deletion, who have received at least one prior therapy.[1]

More than 30 years ago, BCL-2 proteins were discovered to be master regulators of apoptosis,[2,5-6] the highly regulated process by which the human body disposes damaged and unwanted cells.[7-8] The evasion of apoptosis is a hallmark of cancer,[9] and its impairment is a key step in tumor initiation and progression. BCL-2 proteins are antagonists of pro-apoptotic proteins and are frequently overexpressed in cancers, and are implicated in driving both tumor growth as well as resistance to chemotherapies.[10-13] As a therapeutic target, it stood to reason that small molecule inhibition of BCL-2 should lead to disruption of those detrimental protein-protein interactions and restore apoptotic function. Herculean and innovative efforts by the medicinal chemistry team at AbbVie (previously known as Abbott) spanning more than twenty years of research[14-17] ultimately demonstrated the proof-of-concept that BCL-2 was a viable target for treating heme malignancies which subsequently led to the discovery of **1**, as a BCL-2 selective inhibitor.

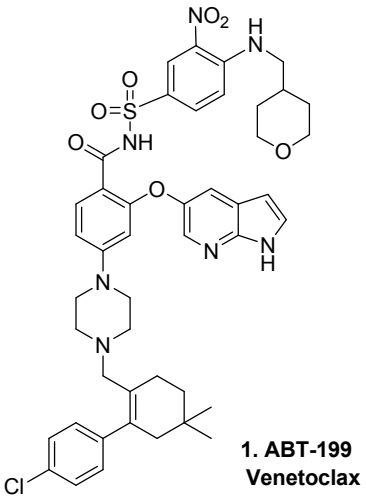

Figure 1. Venetoclax 1 (ABT-199)

A first generation synthesis adapted from the medicinal chemistry route was rapidly developed to produce multi-kilogram quantities of **1**. However, this route still was inefficient and involved significant operational challenges as well as low overall yield and throughput. By strategically

redesigning the synthesis and implementing a Buchwald-Hartwig amination, the new synthetic route successfully addressed the chemistry challenges associated with the first generation route and improved the process convergence, overall yield and manufacturing robustness. This article will discuss an enhanced, robust process for synthesizing **1** with consistently high quality..

2. FIRST GENERATION LARGE-SCALE SYNTHESIS

In general, developing an optimized chemical process for a drug candidate requires substantial amounts of time and resources, which may not be appropriate for the early stages of development as the physical supply of API is often on the critical path. Expeditious delivery of sufficient quantities of API to enable advancement of a program oftentimes takes priority, especially considering the high attrition rate in early development prior to demonstrating proof-of-concept and intended efficacy.[18] With this in mind, an initial assessment of the synthetic route indicated that the quickest path to the development of a scalable process for the complex drug candidate **1** was to improve upon the existing medicinal chemistry approach (Scheme 1).[19]

Scheme 1. Medicinal Chemistry Approach to 1

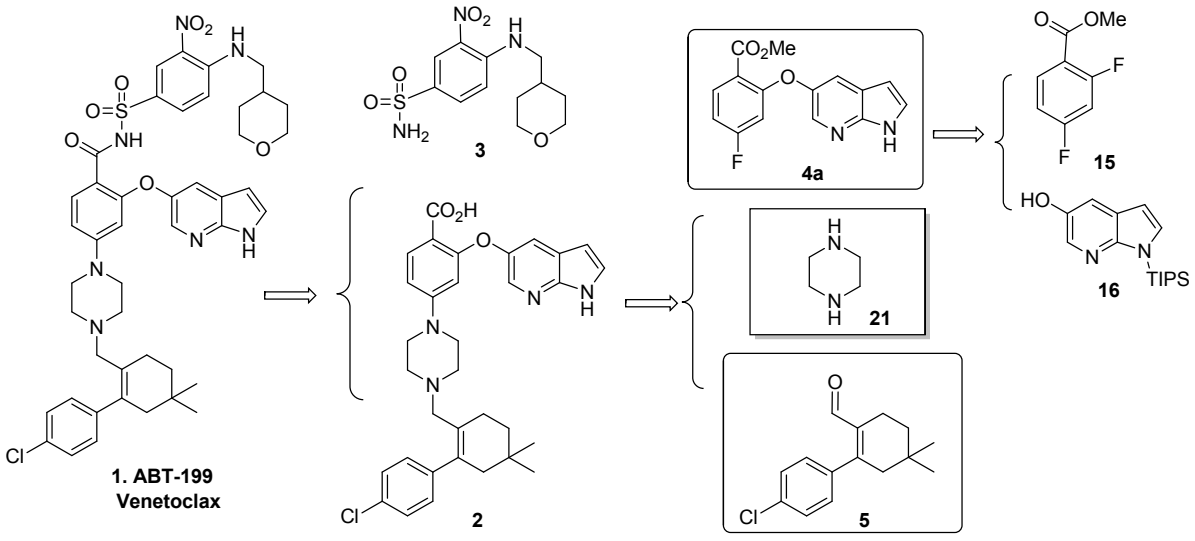

In the medicinal chemistry synthesis, the final coupling of the core acid **2** and the sulfonamide **3** worked reasonably well. However, the S_NAr reaction for the key building block **4a** had regio and chemoselectivity concerns, and it also suffered from reproducibility issues caused by strong scale-dependence of agitation; the synthesis of the key aldehyde intermediate **5** was lengthy and included tedious purification. Additionally, the aldehyde **5** was a thick syrup, which made the isolation of acceptable quality material difficult for large-scale production. Early process chemistry efforts were therefore focused on improving these problematic and inefficient reactions and isolations, and to overcome scale-up challenges associated with the medicinal chemistry synthesis.

The initial synthesis of the aldehyde intermediate **5**[19] was accomplished with a five-step reaction sequence (Scheme 2) starting from 3,3-dimethylcyclohexanone **6**. First, the ketone **6** was converted to **7** by a Claisen condensation with dimethyl carbonate. Intermediate **7** was then converted to vinyl triflate intermediate **8** which underwent a Suzuki cross-coupling reaction with boronic acid **9** to produce the ester intermediate **10.** Reduction of the ester **10** with $LiBH_4$ led to the alcohol **11** which was oxidized to aldehyde **5** using Dess-Martin periodinane. Silica gel column chromatography was required to purify the aldehyde **5** to achieve the desired purity profile.

Scheme 2. Medicinal Chemistry Route for Aldehyde 5

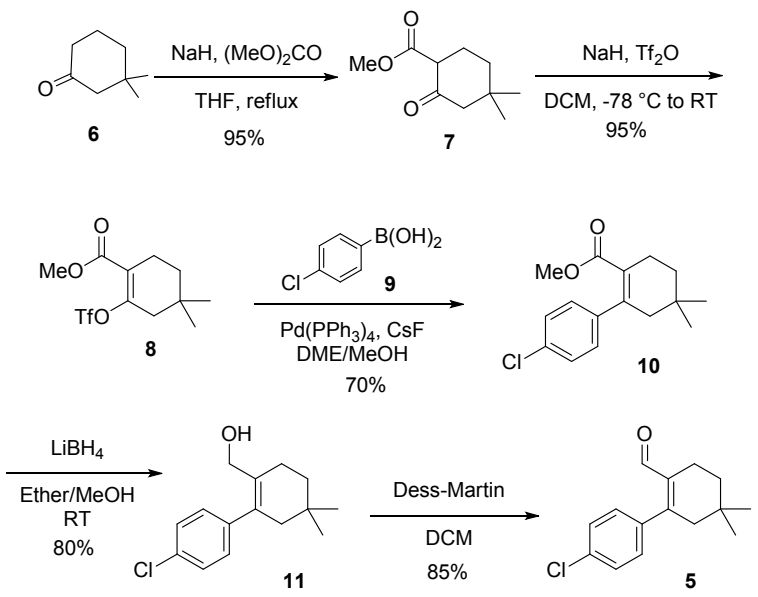

A two-step, one-pot synthesis of aldehyde intermediate **5** (Scheme 3)[20] was developed as a streamlined alternative. Starting with the same starting material 3,3-dimethylcyclohexanone **6**, the ketone was converted to the chloro-aldehyde intermediate **12**, which was directly subjected to the Suzuki coupling with boronic acid **9** without need for isolation. Aldehyde **5** was isolated in 37% yield over the two steps after column chromatography purification.

Scheme 3. A New Synthesis for Aldehyde 5

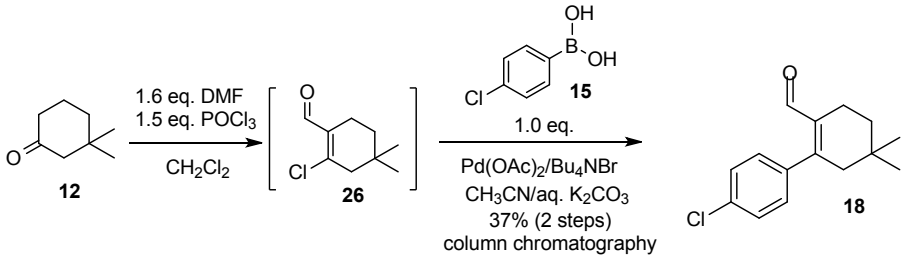

Although the synthesis of the aldehyde **5** was significantly improved from the five-step sequence, its isolation and purification remained challenging due to its syrup-like physical state, which made removal of process impurities difficult. The Suzuki cross-coupling [21] reactions for both the initial and improved syntheses introduced several highly toxic mutagenic and carcinogenic impurities (**9**, **13** and **14** in Figure 2) which required control to part per million

(ppm) and part per billion (ppb) levels in drug substance, respectively.[22] Consequently, purification to reduce these impurities to desirable levels required tedious column chromatography.

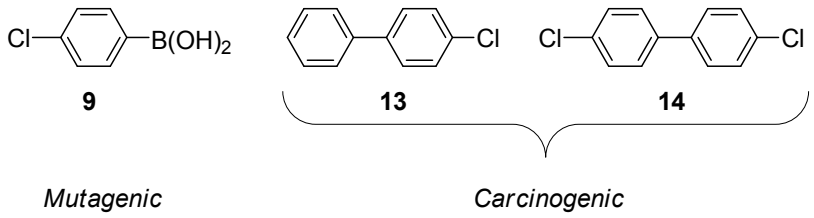

Figure 2. Mutagenic and Carcinogenic Impurities Generated from the Aldehyde Synthesis

In an effort to eliminate the chromatographic purification, attempts were made to form a crystalline bisulfite adduct of aldehyde **5**. Although crystallization of the bisulfite adduct was possible, multiple crystallizations were required to achieve the desired purity profile, resulting in substantial product losses. The significantly higher isolated yield of **5** from chromatography led us to proceed with this method of purification in spite of the resource and time-intensity required.

The initial S_NAr reaction involved reacting methyl 2,4-difluorobenzoate **15** with N-triisopropylsilyl-protected hydroxylazaindole **16** (Scheme 4).[23] Investigation of this reaction revealed that substantial levels of desilylation occurred during the reaction and produced a mixture of products with and without the TIPS protecting group. The mixture of products could be converted to the desired intermediate **4a** by treatment with TBAF. The major byproducts were **17** and **18**, generated from non-regioselective displacement of the 4-fluoro group; interestingly, only a minimal amounts of byproduct **19**, from *N*-arylation of the deprotected azaindole, was observed.

Scheme 4. Initial S_NAr Reaction Using the TIPS-Protected Azaindole 16

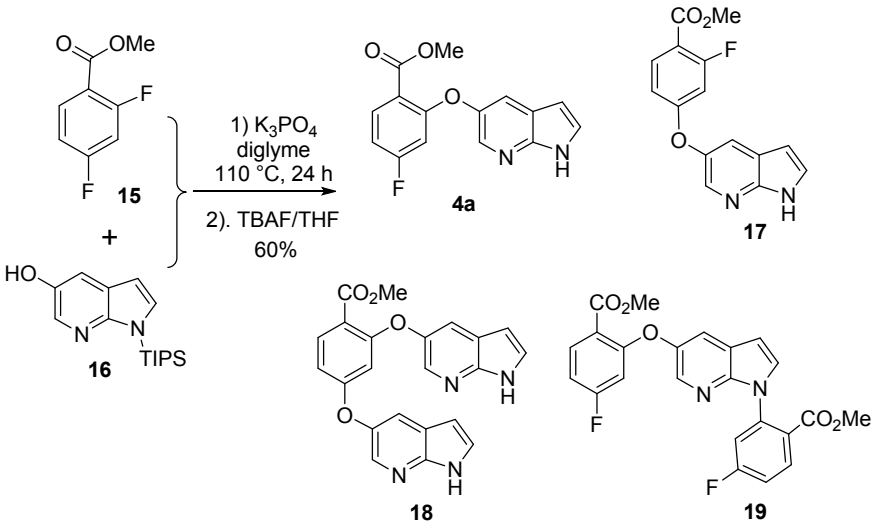

Based on this observation, we reasoned that the protection/deprotection steps could be completely avoided and the S_NAr reaction could be performed using the unprotected azaindole **20** (Scheme 5). Conditions for the S_NAr with azaindole **20** were briefly screened; after evaluating solvent, base and reaction temperature, it was found that the reaction conditions using a combined solvent system of 2-Me-THF/DMF (10:1) with KO*t*-Bu afforded comparable results to the original chemistry using TIPS-protected **16**.

Scheme 5. The New S_NAr Using unprotected azaindole 20

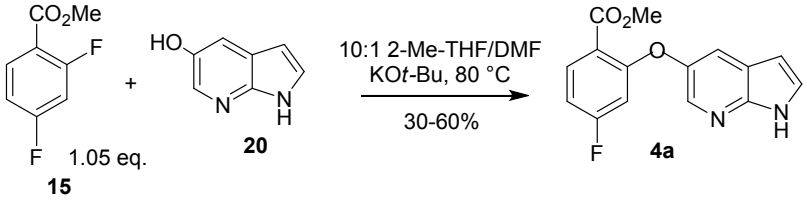

During the scale-up of this S_NAr reaction, the product purity profile was discovered to be extremely sensitive to agitation and is heavily scale-dependent, because the reaction mixture started off as a heterogeneous mixture due to the low solubility of **20**. On 2-kg scale, the reaction proceeded similarly to lab experiments in respect to the yield and product purity profile. However, when the reaction scale was increased 10-fold, a substantial increase of the undesired

byproducts was observed, which are from the S_NAr at the 4- position and the double S_NAr at both 2 and 4-positionresulting in a significantly diminished yield of 33%. Chemical engineering studies to understand the agitation power in relation to the reactor geometry was modeled, but reproducibility challenges with respect to product purity profile and yield persisted.

The second S_NAr reaction of **4a** with piperazine **21** (Scheme 6) for the preparation of intermediate **22a** was initially carried out at 100 °C in DMSO,[24] but the safety evaluation of this reaction revealed that exothermic decomposition of the reaction mixture occurs at 200 °C with an onset temperature at 130 °C. To address this safety concern for manufacture, the reaction temperature could be reduced to 50 °C while still achieving full reaction conversion in ≤10 h.

Scheme 6. The S_NAr Reaction for Intermediate 22a

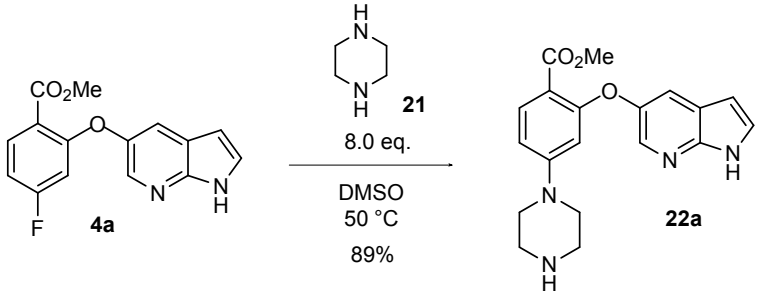

As expected, the dimeric impurity **22b** (Figure 3) was also generated during the reaction and needed to be controlled to <0.5% in the isolation of **22a** due to limited purge in the downstream steps. The initial conditions using 4 equivalents of piperazine **21** produced about 3% of dimer with about 3-4% of starting material **4a** remaining. When the amount of piperazine was increased to 8 equivalents, the amount of the dimer was significantly reduced to ~0.4%; further increasing the equivalents of piperazine diminished the amount of dimer formed, but was not necessary as the target limit of the impurity was achieved.

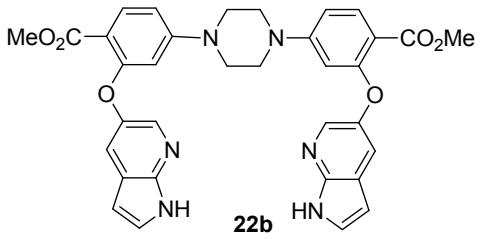

Figure 3. The Dimer Impurity from the Step 1 of Scheme 4

Minimal process optimization effort was directed to the reductive amination for the preparation of **23a** as the initial conditions were efficient. Coupling of piperazine derivative **22a** and aldehyde **5** was achieved using sodium triacetoxyborohydride at 20 °C to give 82% yield of **23a**. Notably, the reaction required more than10 h to achieve full conversion when <1.3 equivalents of $NaBH(OAc)_3$ was used; however, while increasing the amount of $NaBH(OAc)_3$ did reduce the reaction time, it had the undesired effect of increasing the levels of competitive aldehyde reduction to alcohol **11**.

The sulfonamide **3** was initially prepared in Discovery Chemistry by the S_NAr reaction of 4-fluoro-3-nitrobenzenesulfonamide **24a** with the THP-amine **25** (Step 4 of Scheme 7).[25] The reaction proceeded well and was carried out at ambient temperature in MeCN. Although bulk supplies of **24a** were unavailable, it could be readily replaced with the less expensive chloro analogue **24b**, but heating to 80 °C was required to effect clean S_NAr (Step 4 of Scheme 4).[20] Since both **24a** and **24b** are strong sensitizing and mutagenic agents, an excess 1.4 equivalents of the amine **25** was used to ensure complete consumption of the starting material.

The saponification of the methyl ester **23a** to the acid **2** and the final coupling reaction of **2** with the sulfonamide **3** with the core acid **2** (Step 5 of Scheme 7)[26] were briefly studied and the initial conditions were used without major modification.

These initial process optimization efforts led to the identification of alternative chemistry for the synthesis of key intermediates with improved scalability and efficiency, but more importantly enabled rapid delivery of API. Using this route (Scheme 7), multi-kilogram quantities of drug substance **1** were prepared, allowing early development of this promising drug candidate to move forward without delay.

Scheme 7. Summary of the First Generation Large-Scale Synthesis of 1

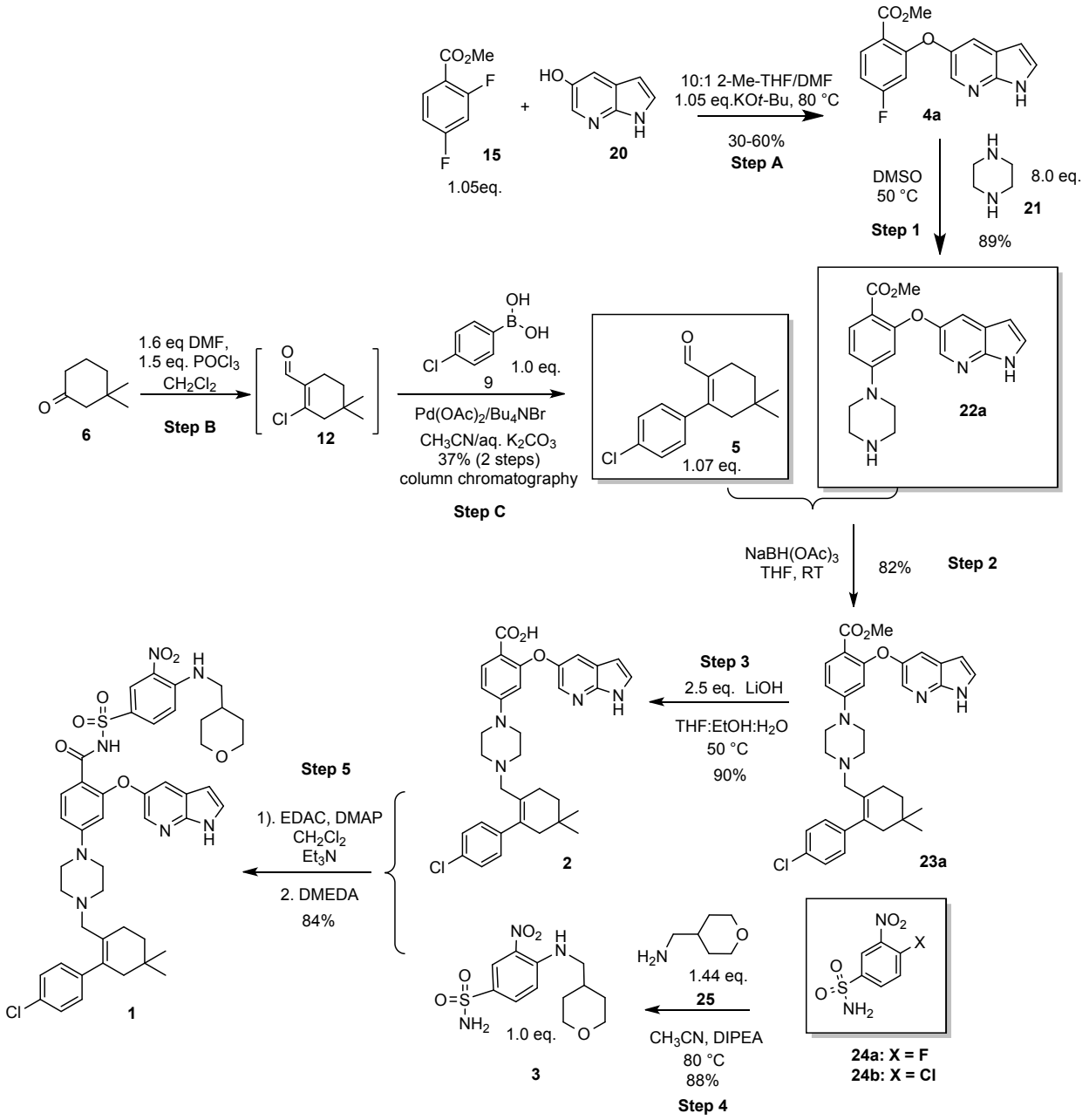

3. RESULTS AND DISCUSSION

Redesign of synthetic route: Following the development of the First Generation Synthesis, the project timeline was significantly accelerated, allowing Process Chemistry only ten months to develop a more scalable and robust synthesis to produce the primary stability batches. [27]

To develop a new synthesis under this compressed timeline, several key considerations for an optimized manufacturing process had to be assessed and prioritized. Reaction safety, process robustness, cost and labor effectiveness, facile impurity rejection, and environmental impact were the most important considerations. Another key aspect of developing a scalable synthesis is the strategic designation of regulatory starting materials (RSM);[33] the RSMs should have good chemical stability and desirable physical properties with a well-defined impurity profile and should not be a major contributor to impurities in the API.

The first generation synthesis (Scheme 7) did not meet these criteria due to several major concerns: (1) low overall yield and throughput resulting in high cost of drug substance, (2) poor robustness of the S_NAr reaction of hydroxyazaindole to produce **4a** due to its poor regioselectivity and extreme scale sensitivity, and (3) poor physical properties of the aldehyde intermediate **5** complicating its isolation and the removal of mutagenic and carcinogenic impurities from the Suzuki coupling.

In considering a more efficient and robust route, we wanted to preserve the sulfonamide coupling as the final step since some process chemistry efforts had already been dedicated to optimizing the process to ensure isolation of high purity API **1**. We thought it would be advantageous to leverage the new 2-step synthesis developed for aldehyde intermediate **5** (Scheme 3). It was also imperative for us to avoid isolation of aldehyde **5** in order to overcome the labor-intensive cumbersome purification and isolation. Finally, we needed to address the robustness concerns of the S_NAr reaction of hydroxyazaindole **20** (Scheme 5) for its poor predictability and reproducibility in producing intermediate **4a** on scale.

With these objectives in mind, retrosynthetic analysis of the core ester **23a** was performed (Scheme 8). The key disconnection involved assembly of ester **23a** either by a Buchwald-Hartwig amination between the intermediate **4b** and **26** or a S_NAr reaction of **4a** with **26**. The new piperazine intermediate **26** could be prepared from the reductive amination of aldehyde **5** with *N*-Boc-piperazine followed by boc-deprotection. This new reaction sequence could avoid the isolation of aldehyde intermediate **5** and potentially furnish a crystalline intermediate.

Scheme 8. Retrosynthetic Analysis of the Proposed New Synthesis

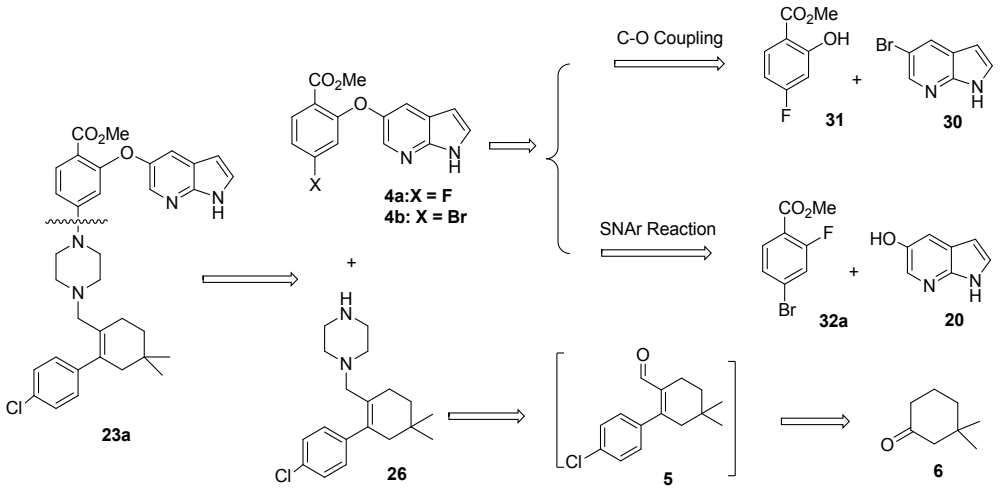

The 4-fluorobiaryl ether **4a** could arise from a C-O cross-coupling reaction of the 5-bromoazaindole **30** with 2-hydroxy-4-fluorobenzoate **31**. Alternatively, the 4-bromobiarylether **4b** could be prepared by a regioselective S_NAr reaction of methyl 2-fluoro-4-bromobenzoate **32a** with 5-hydroxyazaindole **20**. In this case, the cost and availability of **32a** would have to be addressed as it was expensive and unavailable in bulk quantities.

Proof-of-concept studies for the new route started with the evaluation of the alternate synthesis for **4a**. A variety of C-O cross-coupling reaction of **30** and **31** with both palladium and copper

catalysts were evaluated and resulted in no desired product formation (Scheme 9). [28] We attributed the poor reactivity to the poor nucleophilicity of electron-deficient phenol **31**.

Scheme 9. Alternate Synthesis for Biarylether 4a via C-O Cross-Coupling

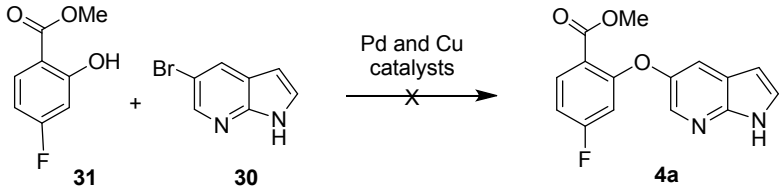

We then turned our attention to evaluating the alternate regioselective S_NAr reaction of **32a** and **20** (Scheme 10). With the introduction of the bromide at the 4- position, differentiating its reactivity from the 2-fluoro, we no longer encountered any regioselectivity issues. In fact, the S_NAr reaction of 5-hydroxyazaindole **20** with **32a** using NaO*t*-Bu in DMF[20] proceeded cleanly and the desired product **4b** was obtained in high yield (>86%) as a crystalline solid.

Scheme 10. New S_NAr Reaction for Bromobiarylether 4b

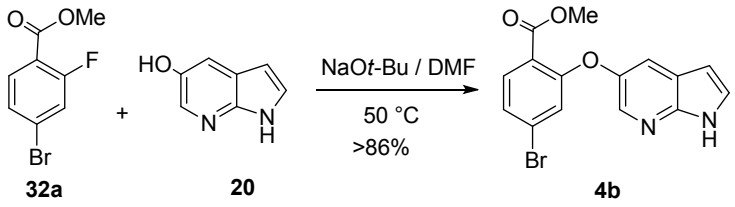

A new reaction sequence for the preparation of **26** that avoids the isolation of aldehyde **5** was evaluated (Scheme 11). The crude aldehyde **5** underwent clean reductive amination with *N*-Boc-piperazine **28** to form the piperazine intermediate **29** in 74% yield over 3 steps with high purity (>98%).[20] The desirable physical property of **29** as a crystalline solid enabled thousand-fold reduction of the mutagenic and carcinogenic impurities (**9**, **13** and **14** in Figure 2) by

crystallization. Additionally, deprotection of the Boc group using an aqueous hydrochloric acid solution produced chloropiperazine **26** as a crystalline bis-HCl salt in 96% yield, further enabling the purge of process impurities. The new reaction sequence for **26** produces higher overall yield and affords robust control for rejection of impurities, but most notably avoided the need to handle and isolate the syrup-like aldehyde intermediate **5** which had previously required tedious column chromatography purification.

Scheme 11. Alternate Synthesis of Chloropiperazine 26

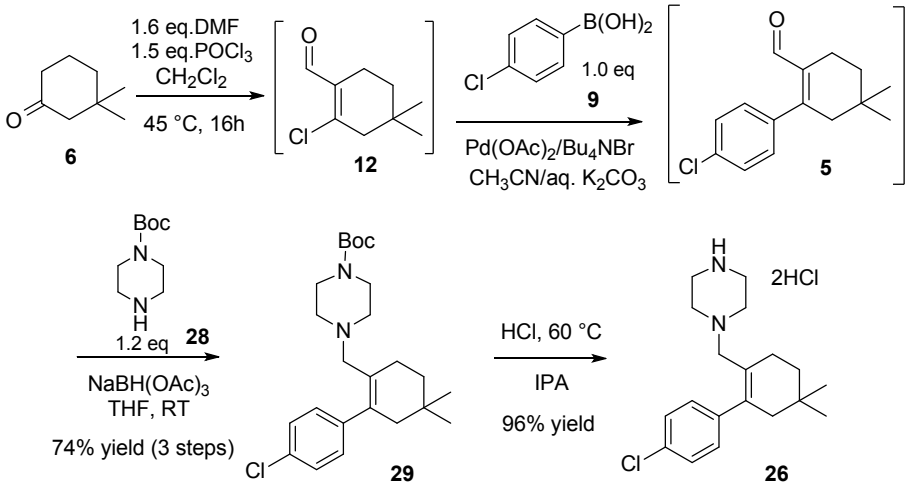

The new syntheses developed for the key building blocks **4b** and **26** provided sufficient quantities of materials for investigation of the Buchwald-Hartwig amination.[29] The coupling was initially evaluated with a variety of catalysts with methyl ester **4b**; however, C-N bond formation was relatively inefficient and substantial amounts of byproducts were formed. The two major byproducts were the piperazine amide from transamidation and the 4-bromobenzoic acid from saponification of the methyl ester. A minor amination byproduct was the result of C-N coupling at the aryl chloride, indicating there could be potential chemoselectivity issues (i.e. oxidative

addition into Br vs Cl). Observation of the ester-related byproducts from the initial set of experiments led us to switch to the more sterically hindered *tert*-butyl ester **4c**, which we hypothesized should be less prone to transamidation as well as saponification. Indeed, when *tert*-butyl ester **4c** was used in the coupling reaction, very little transamidation and saponification were observed. Our most promising initial result was with a high catalyst load of $[Pd(P(t\text{-}Bu)_3)Br]_2$ (20 mol% of total Pd),[29-30] the reaction proceeded with high conversion (>99%) and high yield (>93%). It was found that >3 equivalents of NaO*t*-Bu were required (Scheme 12).

Scheme 12. Initial Buchwald-Hartwig Amination for 23c

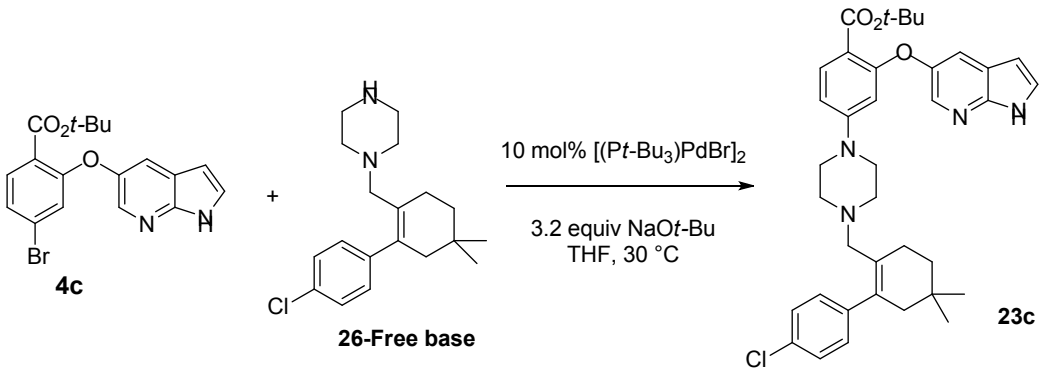

To develop a cost effective manufacturing process, the attempts were made to lower the Pd catalyst loading for the C-N coupling. When the amount of $[Pd(P(t\text{-}Bu)_3)Br]_2$ used was reduced to 1 mol% (for 2 mol% of total Pd), the reaction conversion stalled out at ~40% when 3.2 equivalentsof NaO*t*-Bu were used (Figure 4). However, full conversion (>99%) could be achieved with larger excesses of base (~7 equivalents); we noted that less NaO*t*-Bu was required with higher Pd loadings. At present, we hypothesize this phenomenon is a result of unidentified, but subtle organometallic interactions;.the π-basic N-1 and N-7 of the azaindole may complex to Pd to form catalytically inactive, off-cycle Pd—N species and the excess NaO*t*-Bu may be necessary to recover the catalyst via a Pd alkoxide.[31] Previously reported methods for

aminations with LiHMDS in the presence of similar unprotected heterocycles gave poor conversion in our case.[30e-f] Use of a large excess of NaO*t*-Bu in this coupling reaction has little impact to the overall cost of goods as NaO*t*-Bu is relatively inexpensive and could be readily sourced.

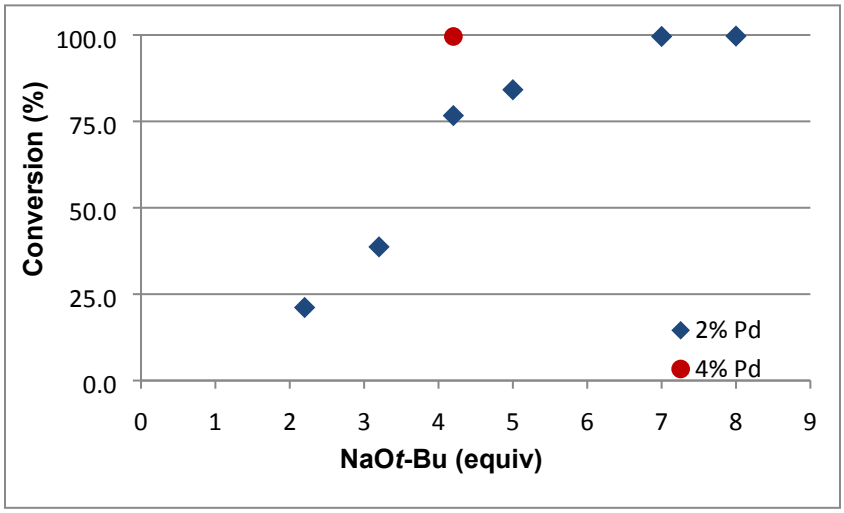

Figure 4. Impact of NaO*t*-Bu Equivalents on C-N Coupling Conversion

The final saponification of the *tert*-butyl ester **23c** turned out to be more challenging than expected, the previous saponification conditions (LiOH in 1:1:1 ratio of THF/EtOH/H_2O at 50 °C) were ineffective for **23c**. The reaction was extremely slow with very little conversion even with extended reaction times. When the reaction temperature was raised, significant amounts of degradation were observed. Other commonly used basic saponification conditions were also examined without success. Switching to acid-mediated conditions with trifluoroacetic acid in dichloromethane or phosphoric acid in acetonitrile gave low yields of product and was accompanied by substantial amounts of decarboxylation. Alternatively, it was found that the *tert*-butyl ester **23c** could be cleanly converted to the methyl ester **23a** under acidic conditions, which subsequently undergoes clean saponification to the desired acid **2** as described before (Step 3,

Scheme 7). Although both reactions proceeded cleanly, this was non-ideal due to the additional step required.

Our analysis of the literature revealed that "anhydrous hydroxide," generated from the reaction of KO*t*-Bu with a carefully controlled stoichiometry of water, could be used to carry out the saponification of a variety of bulky esters in organic solvent.[32] We thought this under-utilized procedure could be promising; and in fact, we observed clean, but incomplete saponification when **23c** was treated under the reported conditions using 2 equivalents of KO*t*-Bu and 1 equivalents of water in THF at room temperature. After some optimization, the reaction proceeded to completion to give acid **2** in >90% yield when the saponification was performed with 5 equivalents of KO*t*-Bu and 3 equivalents of water at 55 °C (Scheme 13).

Scheme 13. Saponification of t-Butyl Ester with "Anhydrous hydroxide"

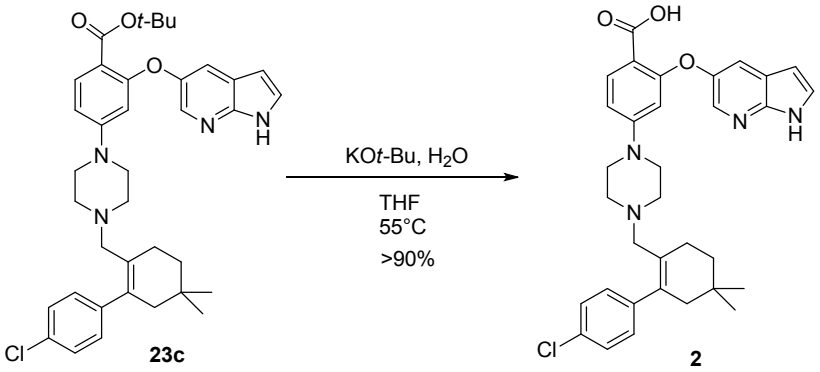

Having demonstrated that the Buchwald-Hartwig coupling could be used to successfully prepare **23c**, a cost effective synthesis of key intermediate **32c** was required. As previously mentioned, methyl benzoate **32a** was expensive and unavailable in large quantities and this was also true for the *tert*-butyl analogue **32c**. So, a new synthesis for **32c** that utilizes inexpensive and readily available raw material **33** was developed (Scheme 14).

Selective metalation of 4-bromo-2-fluoro-1-iodobenzene **33** with iPrMgCl affords Grignard intermediate, which was then reacted with Boc_2O at -5 °C to produce the desired *tert*-butyl ester **32c** in 88% yield. A simple aqueous workup afforded product in >98% area purity, which could be used in the following S_NAr reaction without further purification. The timely development of this straightforward and economical synthesis of **32c** provided a reliable source of the starting material and was an important factor in deciding to pursue this new synthetic route.

Scheme 14. New Synthesis for the *tert*-Butyl Ester 32c

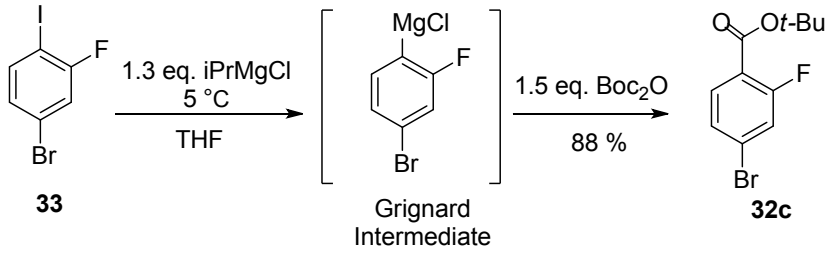

These proof-of-concept studies demonstrated the improved efficiency and convergence of the new synthetic route. A Buchwald-Hartwig amination reaction was used to connect the two key building blocks bromobenzoate **4c** and chloropiperazine **26.** Moreover, highly scalable processes for both **4c** and **26** were implemented. This new synthesis addressed all of the aforementioned challenges associated with the first-generation process, while also importantly reducing the cost of goods. Having achieved the goals set forth, the decision was made to further optimize this route to synthesize **1**.

Process Development of the New Synthesis. Robust control strategies that define the process parameters and operating ranges must be established to ensure consistent process performance and product quality. They are based upon thorough examination and fundamental understanding of each reaction and the corresponding risk assessment. Control of material attributes and purity

profiles for each intermediate and the RSMs[33] are also important parts of the overall strategy and are established based on process understanding of impurity formation and their downstream fate.

The development of a robust manufacture process for **1** was focused on further optimization and understanding of the reactions starting from the designated RSMs (**4c, 26** and **24b**). One of the more important aspects of this endeavor was to optimize and study the Buchwald-Hartwig amination between **4c** and **26**. The first step was to identify a more efficient catalyst. Based on the promising initial result with the $[Pd(P(t\text{-}Bu)_3)Br]_2$ precatalyst, a focused ligand screen was performed by evaluating *tert*-butyl-substituted and other bulky phosphines (Figure 5).

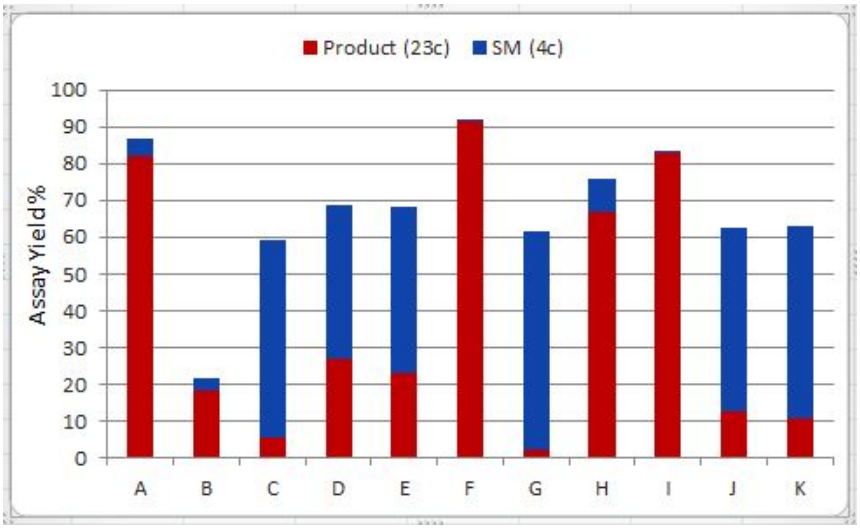

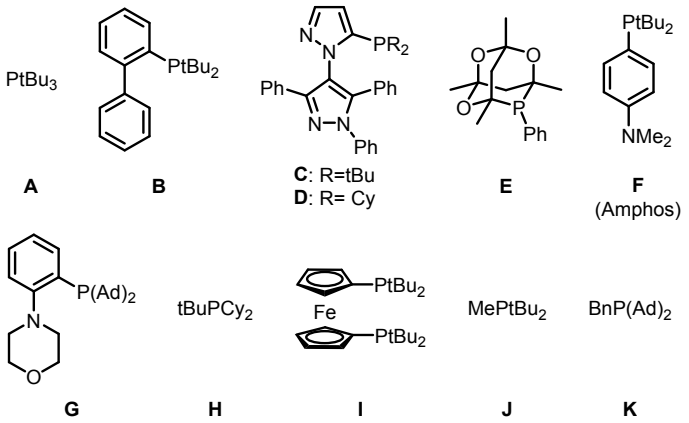

Figure 5. Focused Ligand Screen for C-N coupling

From this ligand screen where 2.0 mol% of total Pd was used, not surprisingly, $PtBu_3$ (A in Figure 5) was still effective, but both Amphos (F) and DiTBPF (I) were also observed to be effective for the coupling of **4c** and **26**, each giving >80% conversion to **23c**. In order to better differentiate among these three ligands, the amination was performed under more challenging conditions, now using only 1.0 mol% of total Pd (Figure 6). Under these stressed conditions, Amphos[29g] was discovered to be the superior ligand (entries F and G in Figure 6). Although $[Pd(\pi\text{-cinnamyl})Cl]_2$ gave a slightly more active catalyst than Pd_2dba_3, due to cost and commercial availability, the decision was made to move forward with the process using Pd_2dba_3.

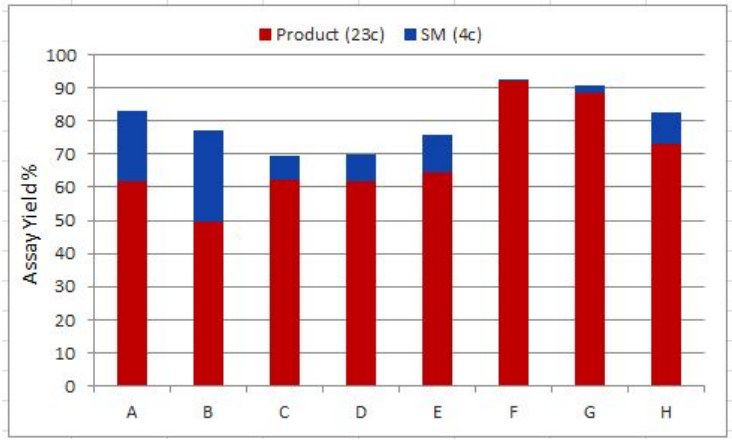

A $[(PtBu_3)PdBr]_2$
B $[\pi\text{-cinnamyl})PdCl]_2 + PtBu_3$
C $Pd(DiTBPF)Cl_2$
D Pd_2dba_3 + DiTBPF
E $Pd(OAc)_2 + PhB(OH)_2$ + DiTBPF
F $[\pi\text{-cinnamyl})PdCl]_2$ + AmPhos
G Pd_2dba_3 + AmPhos
H $Pd(OAc)_2 + PhB(OH)_2$ + AmPhos

Figure 6. Evaluation of Pd Precursors for the Amination

The starting material charge ratio of benzoate **4c** to chloropiperazine **26** was found to be important with respect to formation of impurities. When the chloropiperazine **26** was used in excess, increased levels of Cl-amination impurity **37** was generated from further coupling of **26** with the desired product **23c** (Scheme 15). Although the Pd catalyst reacts preferentially with the aryl bromide at low conversion, while approaching high conversion of bromobenzoate **4c**, the

low concentration of aryl bromide relative to the chloride in **23c** leads to the undesired coupling. Therefore **4c** was used in slight excess (1.04 equivalents) to ensure that the impurity **37** is formed in acceptable level as impurity **37** and its daughter impurities are not readily purged downstream.

Scheme 15. The Key Impurity Generated from the Amination

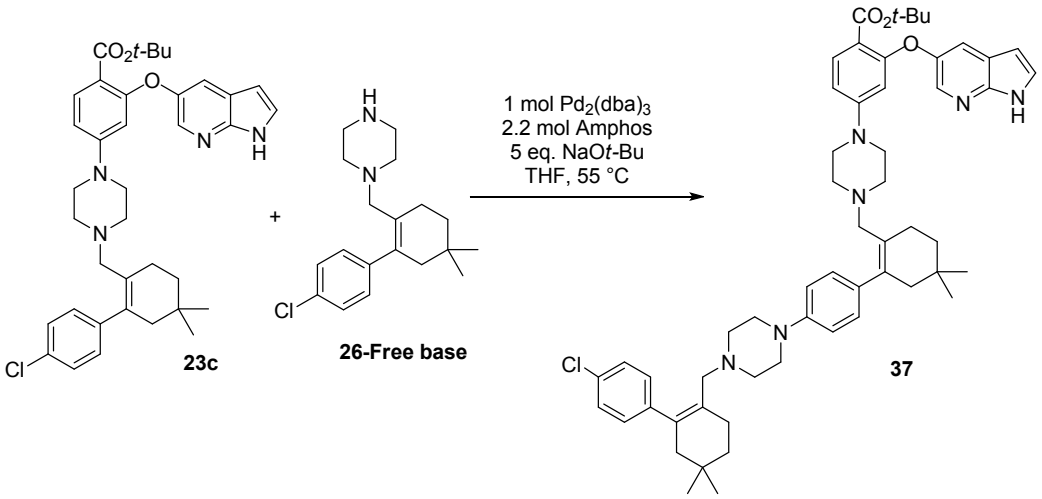

As previously observed, efficient cross-coupling was dependent on the addition of excess equivalents of NaO*t*-Bu and this was also found to be the case with the Pd/Amphos catalyst. However, with 1.5 mol% of the Pd/Amphos catalyst as few as 4 equivalents were necessary to achieve full conversion. It was also observed that the quality of NaO*t*-Bu had a significant impact on the reaction performance as such large amount is used. When old lots of NaO*t*-Bu were used, the reaction proceeded to generate high levels of benzoic acid impurities, from the saponification of both **4c** and **23c**. We assumed that the old lots of base contained higher level of NaOH generated from quenching of NaO*t*-Bu with atmospheric moisture, analogous to the "anhydrous hydroxide" generated in the saponification of the *tert*-butyl ester **23c** to the core acid **2**. Saponification of **4c** generates a sodium carboxylate which in theory could couple with chloropiperazine **26** to give core acid **2** directly; however, due to its poor solubility in THF, the carboxylate does not undergo this amination, so the saponification of **4c** is an unproductive

pathway resulting in lower yield of **23c** and higher levels of impurities. Analytical control of the quality of NaO*t*-Bu to ensure low levels of NaOH would be challenging and impractical, especially given that the base would be re-exposed to atmospheric conditions following the quality testing. Therefore, it was necessary to develop a robust operational control strategy to ensure minimal amounts of NaOH would be introduced to the reaction. Given the very low solubility of NaOH in THF, filtration of the NaO*t*-Bu/THF solutions to remove the sodium hydroxide in laboratory experiments demonstrated that the amination reaction proceeded consistently with lots of varying quality. Incorporation of a filtration unit operation during manufacturing for removal of NaOH was straightforward and offered a practical and robust strategy to enable this sensitive reaction to be carried out reproducibly.

The sensitivity of the coupling reaction to the level of oxygen in the system could adversely affect the reaction performance, producing variable results. This potential concern was addressed by controlling and monitoring the oxygen level of the headspace using an oxygen monitor. It was determined that an oxygen level of ≤40 ppm in the headspace was sufficient to ensure consistent reaction performance and could be achieved by sub-surface sparging of solvents with dry nitrogen and active exchange of reactor atmospheres with vacuum/N_2-purge cycles. With control of the oxygen level, under the optimized conditions (6.5 equivaletns NaO*t*-Bu, 0.8 mol% Pd_2dba_3, 1.6 mol% Amphos in THF) the amination proceeded in >99% conversion with about 90% isolated yield following aqueous workup and crystallization.

The saponification using the "anhydrous hydroxide" was also further studied and optimized. Ultimately, we chose 2-Me-THF as the reaction solvent because it is less hygroscopic than THF, providing better control of water levels in the reaction. In addition, the aqueous work-up and crystallization purification could be performed more effectively in 2-Me-THF. When a series of

saponification experiments were performed with 5 equivalents of KO*t*-Bu and varying amounts of water (Figure 7), the reaction proceeded to completion only when the ratio of water to KO*t*-Bu was ≤1 (i.e. an excess of KO*t*-Bu relative to water). When water was used in excess relative to KO*t*-Bu, incomplete reactions were observed. The optimal molar ratio was determined to be 0.6 using 5 equivalents of KO*t*-Bu.

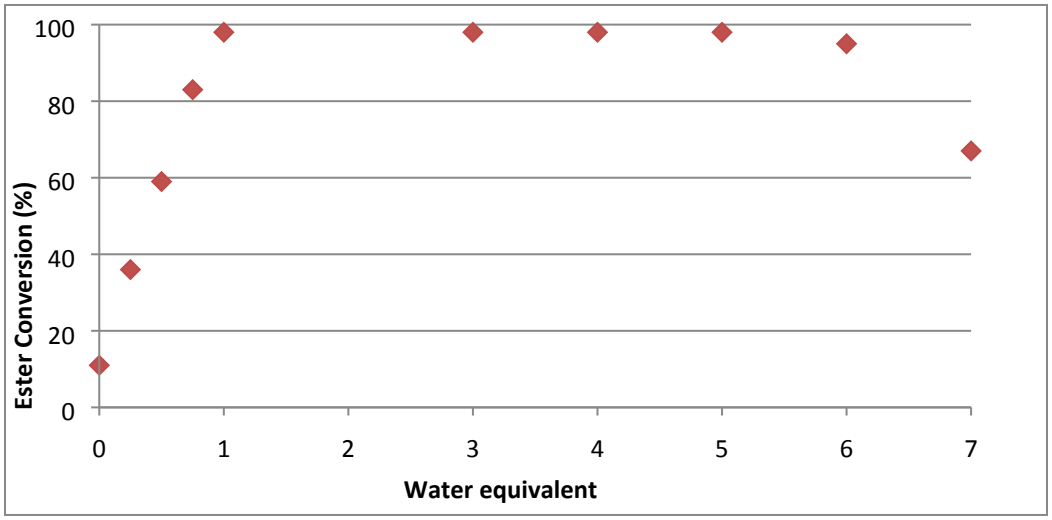

Figure 7. Impact of Water Amount Using 5 equivalents of KOtBu to Reaction Conversion

Higher temperatures drastically reduced the reaction time; the saponification proceeded to completion cleanly within 2 h at 50 °C, while only 43% conversion was achieved during that time period at 21 °C. Since there was no detrimental impact on the impurity profile, the reaction was performed at 50 °C to keep the reaction cycle time low. Under the optimized conditions (6 equivalents KO*t*-Bu and 3.6 equiv H_2O at 50 °C), the reaction proceeded with >98% conversion and ultimately afforded about 90% isolated yield.

Developing robust strategies for the final sulfonamide coupling reaction and isolation was critical to ensure the API quality. The low solubility of the API (**1**) in most organic solvents

limited the solvent options for the amide coupling and isolation. Moreover, the poor nucleophilicity of the sulfonamide resulted in a slow reaction and competing byproduct formation. Screening of coupling of reagents (e.g. CDI, HATU, T_3P and EDAC) and different amine bases (e.g. Hünig's base, Et_3N, DMAP, DBU, DABCO, pyridine, collidine, lutidine, and *N*-methylmorpholine) confirmed that the initial conditions using EDAC and DMAP/Et_3N produced the best results with respect to conversion and purity. Solvent screening revealed that dichloromethane was the optimal solvent and it was also found that the coupling was best run at room temperature. Although increased temperatures (35 °C to reflux) decreased the reaction times, it also increased the levels of impurities.

Efforts were also focused on understanding the formation of impurities and their rejection. Several process impurities were identified and their structures were determined using 2D NMR and MS analyses (Figure 8); the low level impurities **38**, **39** and **40** could be readily removed during aqueous work-up and crystallization. The major bis-amide **41** impurity was difficult to reject and its level varied between batches; it slowly increased during the reaction, meanwhile the reaction rate for forming **1** decreased.

The order of addition of the reagents also impacted the bis-amide impurity level. When EDAC was added last to a suspension of the sulfonamide **3**, core acid **2** and DMAP/Et_3N, the bis-amide **41** was formed in 8%. In contrast, slowly adding core acid **2** to the reaction mixture last resulted in only 5% of the bis-amide. The addition time of the core acid 2 solution also played a key role; longer addition times (8 h) led to incomplete reactions with up to 9.0% of core acid **2** remaining. After a series of experiments (Figure 9), it was determined that the best reaction profile was obtained with slow addition of a mixture of core acid **2** with Et_3N in dichloromethane to a

suspension of sulfonamide **3**, DMAP and EDAC in dichloromethane with an optimal addition time of 2~6 h.

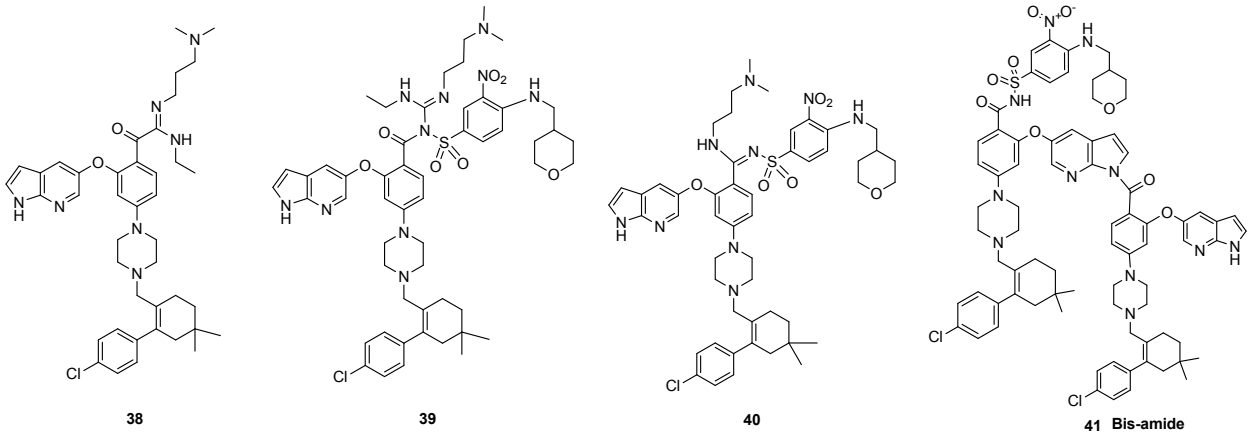

Figure 8. Impurities Generated in the Sulfonamide Coupling Reaction

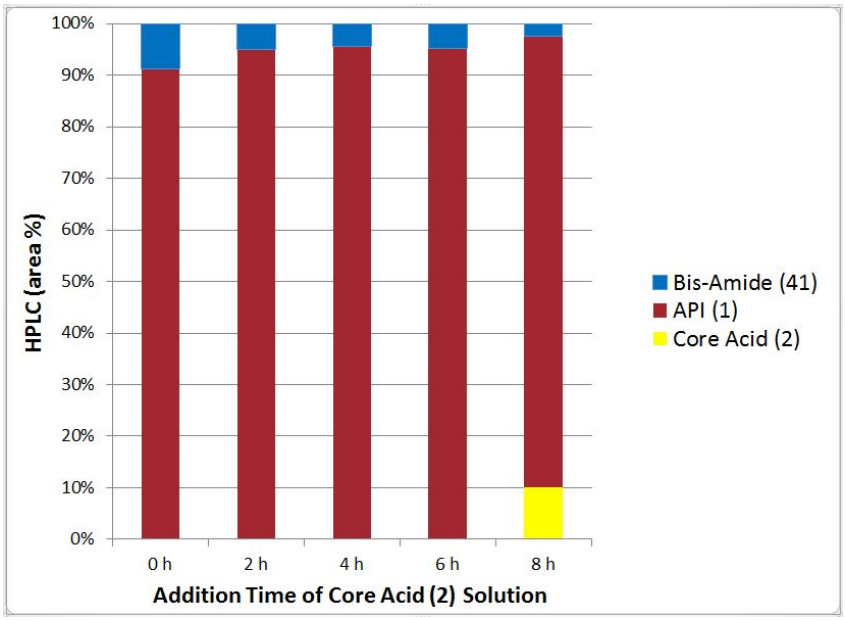

Figure 9. Impact of the Addition Time of the Core Acid (2) Solution

It was also discovered that treatment of bis-amide **41** with *N*,*N*-dimethylethylediamine (DMEDA) led to the re-formation of desired product **1** along with the corresponding DMEDA-

amide impurity **42** which was readily rejected (Scheme 16). This discovery further ensured the process robustness with respect to impurity rejection.

Scheme 16. Derivatization of the Major Dimer API Impurity

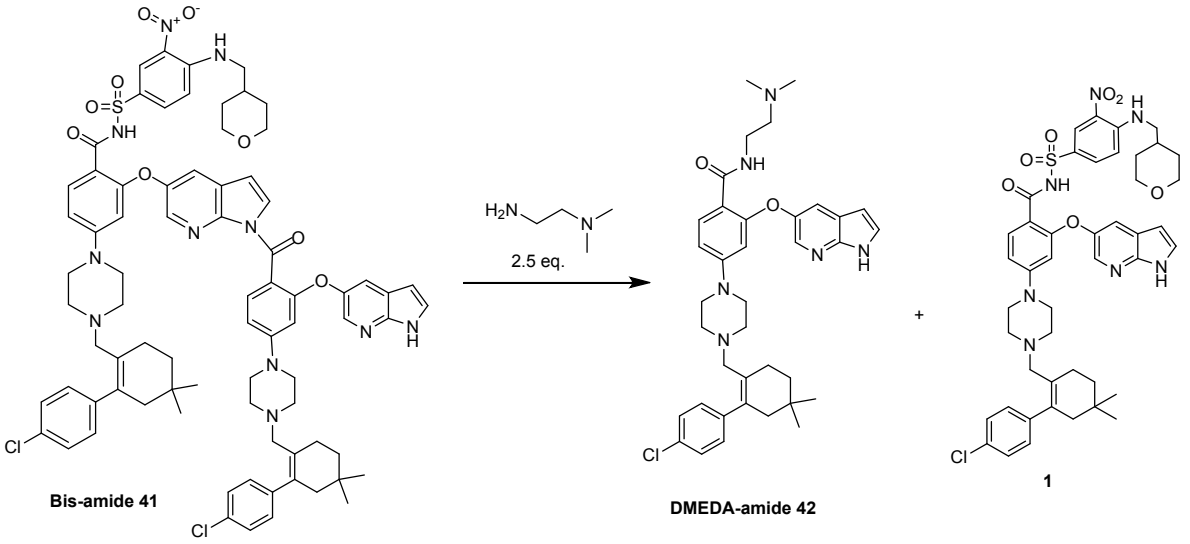

The API **1** was found to readily form solvates which had low solubility, making the work-up of the amide coupling product challenging. After examination of different solvents and solvent mixtures, we opted to use dichloromethane for the work-up and isolation. A dichloromethane solvate was found to spontaneously crystallize from solution during aqueous extractions; therefore the work-up was performed at high dilution (20 L/kg) and at 35 °C to keep the API soluble. In addition, a small amount of methanol (0.5 L/kg) was added to the organic layer after each extraction to increase product solubility and prevent product crystallization. The extractive work-up uses aqueous acetic acid to remove excess DMAP followed by sodium bicarbonate wash to remove residual acetic acid and aqueous wash with 5% NaCl to prevent emulsions.

The final product purification by crystallization effectively rejected product-related impurities and consistently produced **1** in acceptable yield and high quality with desired solid polymorph property. It was achieved by slowly adding ethyl acetate as anti-solvent to attain a 10/1/9 mixture

of dichloromethane/methanol/ethyl acetate, with a targeted total volume of 16 L/kg. As previously mentioned, the addition of methanol (1:10 ratio to dichloromethane) increases the product solubility. Additionally, the presence of methanol also increases the solubility of the reaction impurities and resulted in a robust purification with rejection of up to 5% DMEDA-amide. This optimized process (Scheme 17) has been used for producing **1** with consistent high quality.

Scheme 17. Optimized New Synthesis of 1[20]

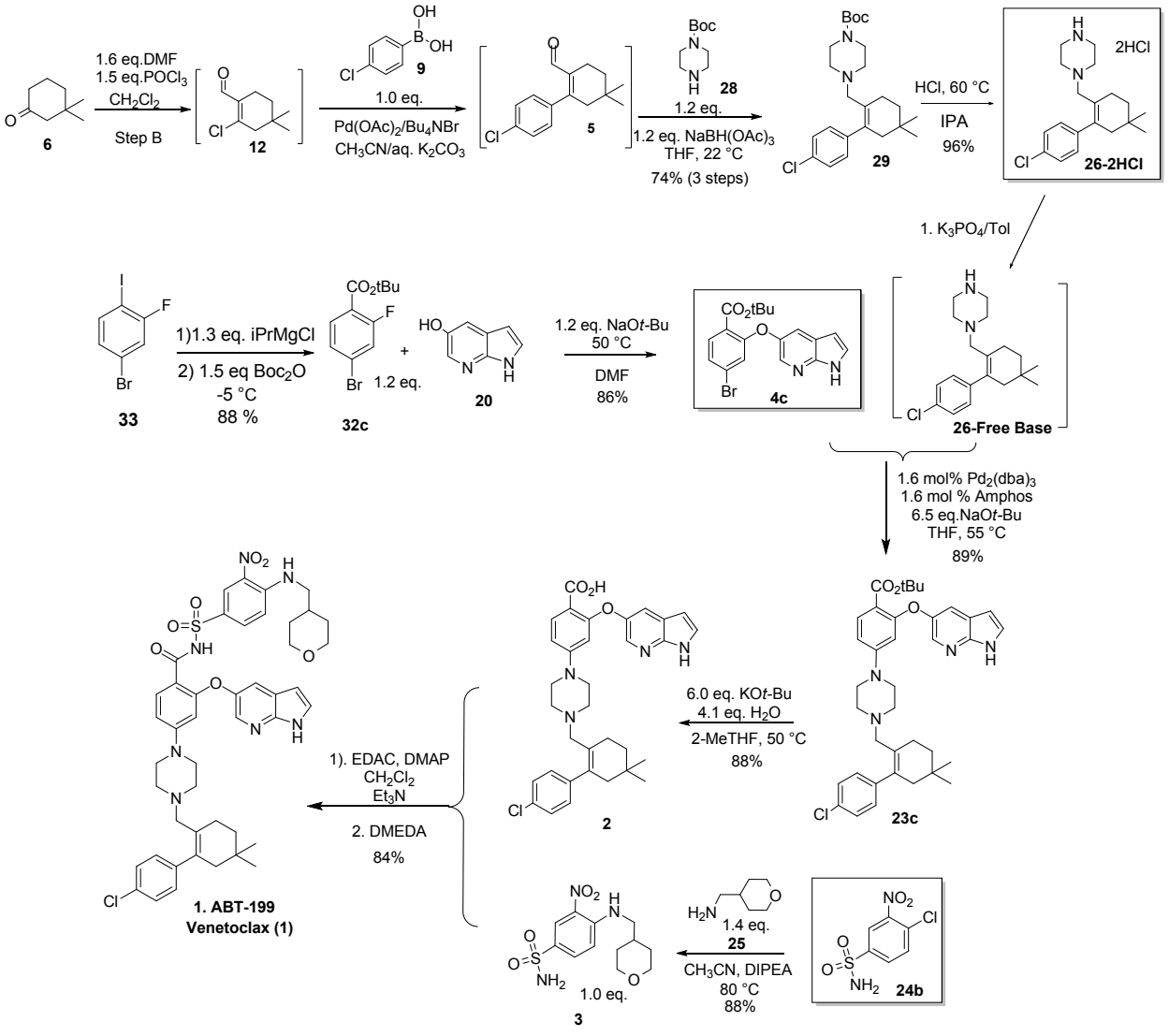

4. SUMMARY

To support the start of clinical development of **1**, early process chemistry efforts were directed towards rapidly developing a scalable synthesis. This first-generation synthesis was based on the medicinal chemistry route, but incorporated several key improvements to address scalability challenges.

A more efficient and robust synthesis that would support increasing demands for API was developed; it offered significant advantages and addressed known scale-up challenges associated with the first-generation synthesis. As was discussed, our convergent second-generation synthesis includes many notable process chemistry innovations: 1) development of a highly efficient and cost-effective synthesis to ensure a reliable supply of key benzoate starting material **32c**; 2) identification of a regioselective and chemoselective S_NAr reaction for key building block **4c** which also overcomes the scale-dependent agitation and reproducibility issues of the initial S_NAr reaction; 3) implementation of a new reaction sequence for the key building block **26,** which circumvented the challenges of handling and isolating a syrup-like aldehyde intermediate **5**; 4) development of a Buchwald-Hartwig amination protocol and control strategy to ensure the execution of this reaction; 5) development of a uniquely effective saponification using anhydrous hydroxide for the highly hindered *tert*-butyl ester **23c**; and, 6) establishing robust protocols and control strategies for the final sulfonamide coupling and the isolation/purification to ensure consistent manufacture of **1**. The newly developed process led to a significant reduction in the cost of goods by more than doubling the overall yield.

5. EXPERIMENTAL SECTION

All commercial reagents and solvents were used without purification. All reactions are carried out under a N_2 atmosphere. The temperatures of the reactions refer to internal temperatures. The reactions were monitored by reverse phase HPLC using spectroscopic grades of acetonitrile and water. The ^{1}H, ^{13}C NMR spectra were recorded on a 400 or 600 MHz spectrometer, with shifts reported in parts per million downfield from tetramethylsilane (TMS) and referenced to residual proton (^{1}H) or deuterated solvent (^{13}C). Melting points were obtained from the corresponding onset point of Differential Scanning Calorimeter (DSC).

Synthesis of *tert*-butyl 4-bromo-2-fluorobenzoate (32c) [20]

To a 300 L reactor were charged with 4-bromo-2-fluoro-1-iodobenzene **33** (15.0 kg, 49.9 mol, 1.0 equiv) and THF (67 kg). The mixture was stirred at 20 °C for 15 min., and the resulting solution was cooled to -5 °C. To the cooled solution was slowly added the 2 M isopropyl magnesium chloride in THF (31.6 kg, d = 0.975 g/mL, 64.8 mol, 1.3 equiv) maintaining the internal temperature below 0 °C. The mixture was stirred at 0 °C for 1 h. To the mixture was slowly added a solution of di-*tert*-butyl dicarbonate (16.4 kg, 75.2 mol., 1.5 equiv) in THF (27 kg) maintaining the internal temperature of no more than (NMT) 5 °C. The solution was mixed at 0 °C for 1 h. The reaction mixture was quenched by addition of 10% citric acid aq. solution (30 kg) slowly maintaining the internal temperature of NMT 20 °C followed by addition of 25% NaCl aq. solution (30 kg). The internal temperature of the quenched mixture was adjusted to 25 °C, and mixed for no less than (NLT) 1 h. The layers were separated. The upper organic layer was concentrated under vacuum to 20 L, and chased three times with THF (27 kg) to a final volume of 25 L. The product solution was filtered and the solid was rinsed with THF (13 kg). The filtrate was concentrated under vacuum to 20 L to obtain a concentrated THF solution of the desired product (**32c**) (18.3 kg, 66 wt.% assayed by HPLC, 88% yield). This product solution

was taken to the next step without further purification. However, a small amount of analytical reference sample was obtained by vacuum distillation to give the desired product as colorless oil: ^{1}H NMR (DMSO-d_6): δ 1.53 (9H, s), 7.50-7.56 (1H, m), 7.68 (1H, dd, J = 10.5, 1.9 Hz), 7.74 (1H, t, J = 8.2 Hz). The proton NMR spectra data for this compound were consistent with authentic compound purchased from commercial source.

Synthesis of *tert*-butyl 2-((1H-pyrrolo[2,3-b]pyridin-5-yl)oxy)-4-bromobenzoate (4c) [20]

To a 300 L reactor were charged with 1*H*-pyrrolo [2,3-b]pyridin-5-ol **20** (5.0 kg, 37.3 mol, 1.0 equiv), *tert*-butyl 4-bromo-2-fluorobenzoate **32c** (17.9 kg, 66wt.%, 42.9 mol, 1.2 equiv), and anhydrous DMF (49 kg). The mixture was stirred at 20 °C for 15 min, and the resulting solution was cooled to 0 °C. To this solution was added a solution of KO*t*-Bu (5.0 kg, 44.5 mol, 1.2 equiv) in DMF (21 kg) slowly maintaining the internal temperature of NMT 5 °C. After addition, the reaction mixture was stirred at 5 °C for 1 h, heated to 55 °C, and stirred for NLT 7 h until the starting material **20** was consumed monitored by HPLC. After the reaction was completion, the reaction mixture was cooled to 20 °C and water (75 kg) was added slowly maintaining the internal temperature of NMT 25 °C (slightly exothermic). The resulting product slurry was mixed at 25°C for 2 h. The crude product was collected by centrifugation and washed with water (24 kg). The crude product, EtOAc (135 kg), and water (36 kg) were then charged back to the reactor. The biphasic mixture was stirred at 25 °C for NLT 30 min until all solids were dissolved. The upper organic solution was separated and concentrated to 50 L. To the solution was added more EtOAc (50 kg) and the solution was concentrated again to 50 L to remove water. The resulting mixture, containing some solid, was heated to reflux to achieve a clear solution; heptane (59 kg) was added slowly at 78 °C. The resulting mixture was stirred at 78 °C for 30 min, and then cooled down to -10 °C at a rate of 10 °C/h. After mixing at -10 °C for 2h, the

product was collected by centrifugation and rinsed with heptane (11 kg). The wet cake was dried under vacuum at 50 °C for 24 h to give 12.5 kg (86%) of the desired product **4c** as an off-white solid: mp: 189.0 °C; MS-ESI (m/z): 389.0 (M+l); ^{1}H NMR (DMSO-d_6): δ 1.40 (9H, s), 6.41 (1H, dd, J = 3.4,1.7 Hz), 7.06 (1H, d, J = 1.8 Hz), 7.40 (1H, dd, J = 8.3,1.8 Hz), 7.51(1H, t, J = 3.4 Hz), 7.58 (1H, d, J = 2.6 Hz), 7.66 (1H, d, J = 8.3 Hz), 8.03 (1H, d, J = 2.7 Hz), 11.72 (1H, s).

Synthesis of 2-chloro-4,4-dimethylcyclohexanecarbaldehyde (12) [20]

To a 200 L reactor were charged with DMF (12.2 kg, 166.9 mol, 1.6 equiv) and CH_2Cl_2 (40 kg) followed by slow addition of $POCl_3$ (24.7 kg, 161.1.0 mol%., 1.5 equiv) slowly maintaining the internal temperature at NMT 5 °C. The resulting solution was warmed to 20 °C and stirred for 1 h. To the solution was added 3,3-Dimethylcyclohexanone **6** (13.5 kg, 107.0 mol, 1.0 equiv.) slowly maintaining the internal temperature at NMT 20 °C. The reaction mixture was then heated to reflux and mixed for NLT 10 h until the starting material **6** was consumed monitored by GC. After the reaction completion, the reaction mixture was cooled to 20 °C and quenched slowly into another reactor that contains a mixture of the 10% NaOAc-7% NaCl aq. solution (84 kg) and CH_2Cl_2 (47 kg) maintaining the internal temperature at NMT 10 °C. The quenched reaction mixture was warmed up to 25 °C and diluted with water (18 kg). The lower organic phase was separated, and the upper aqueous phase was extracted with CH_2Cl_2 (18 kg). The combined organic layers were washed with a 3% K_3PO_4-8% NaCl aq. solution (80 kg). The organic phase was concentrated under vacuum to 40 L, and chased with CH_3CN (21 kg) two times to 25L. The product solution of **12** (18.5 kg, assuming a 100% yield for charge calculation in next step) was used directly in the next step without further purification. A small amount of reference sample was obtained by removing residual solvent(s) under vacuum to give

intermediate **12** as brown oil: ^{1}H NMR ($CDCl_3$): δ 0.98 (6H, s), 1.43 (2H, t, *J* = 6.4 Hz), 2.31 (2H, tt, *J* = 6.4, 2.2 Hz), 2.36 (2H, t, *J* = 2.2 Hz), 10.19 (1H, s).

Synthesis of 2-(4-chlorophenyl)-4,4-dimethylcyclohex-l-enecarbaldehyde (5) [20]

To a 250L reactor were charged with tetrabutylammonium bromide (34.5kg, 107.0 mol., 1.0 equiv.), 4-chlorophenylboronic acid (16.8 kg, 107.0 mol., 1.0 equiv.), and all of the product solution of 2-chloro-4,4-dimethylcyclohex-l-enecarbaldehyde **12** (18.5 kg, 107.0 mol, 1.0 equiv.) from the previous step. The mixture was stirred at 20 °C for 15 min followed by addition of 28% K_2CO_3 aq. solution (145 kg). The mixture was evacuated and purged with N_2 for three times, to the mixture was then charged $Pd(OAc)_2$ (60 g, 0.27 mol, 0.25 mol %) all at once under N_2. The reaction mixture was heated to 30 °C and stirred for NLT 16 h under N_2 until the starting material **12** was consumed monitored by HPLC. Upon the reaction completion, the reaction mixture was cooled to 20 °C. The lower aqueous phase was separated. The upper organic phase along with some intermediate phase were filtered through a layer of the filter aid, and the solid was rinsed with toluene (96 kg). The resulting organic solution was washed first with 12% NaOH aq. solution (62 kg), and then 5% $NaHCO_3$-2% *L*-cysteine aq. solution (55 kg). The organic solution was concentrated under vacuum to 65 L, and chased with toluene (70 kg) to 75L. The product solution was used directly in the next step without isolation (26.6 kg, assuming a 100% yield for charge calculation in next step). A small amount of reference sample was obtained by silica gel column chromatography to give the desired product **5** as brown oil: ^{1}H NMR ($CDCl_3$): δ 1.00 (6H, s), 1.49 (2H, t, *J* = 6.6 Hz), 2.28 (2H, t, *J* = 2.1 Hz), 2.38 (2H, m), 7.13 (2H, m), 7.34 (2H, m), 9.47 (1H, s).

Synthesis of *tert*-butyl 4-((4'-chloro-5,5-dimethyl-3,4,5,6-tetrahydro-[1,1'-biphenyl]-2-yl)methyl) piperazine-1-carboxylate (29) [20]

To a 500 L reactor were charged with all of the solution of 4' chloro-5,5-dimethyl-3,4,5,6-tetrahydro-[1,1'-biphenyl]-2-carbaldehyde **5** from the previous step (26.6 kg, 107.0 mol, 1.0 equiv.), *N*-Boc-piperazine **28** (24.8 kg, 133.1 mol%, 1.2 equiv.), toluene (60 kg), and anhydrous THF (118 kg). The resulting solution was stirred at 20 °C for 5 min. Sodium triacetoxyborohydride (27.2 kg, 128.3 mol., 1.2 equiv.) was added in portions under N_2 maintaining the internal temperature at 25°C. The mixture was stirred at 20 °C for NLT 6 h or until the starting material **5** was consumed monitored by HPLC. The reaction mixture was then quenched by slow addition of 10% citric acid aq. solution (140 kg) at 25 °C, the resulting mixture was stirred for 1h. The upper organic phase was separated and washed with 10% citric acid aq. solution (140 kg). The organic layer was then washed with 4% $NaHCO_3$ aq. solution (140 kg) followed by 25% NaCl aq. solution (140 kg). The product solution was concentrated under vacuum to 80 L, filtered through a layer of filter aid, and rinsed with toluene (20 kg). The combined filtrate was further concentrated under vacuum to 40 L, followed by addition of CH_3CN (160 kg). The resulting mixture was heated to the reflux to achieve a clear solution, and cooled down to -10°C at a rate of 10 °C/h. The product slurry was mixed at -10 °C for 6 h, collected by centrifugation, and rinsed with pre-cooled CH_3CN (30 kg). The solid was dried under vacuum at 50 °C for NLT 12 h to give 33.0 kg (74% three-step yield from **6**) of the desired product **29** as a white solid: mp: 110.8 °C; MS-ESI (m/z): 419.3 (M+1); ^{1}H NMR ($CDCl_3$): δ 1.00 (6H, s), 1.46 (9H, s), 1.48 (2H, t, J = 6.5 Hz), 2.07 (2H, br, s), 2.18 (4H, m), 2.24 (2H, t, J = 6.4 Hz), 2.80 (2H, s), 3.38 (4H, m), 6.98 (2H, m), 7.29 (2H, m).

Synthesis of 1-((4'-chloro-5,5-dimethyl-3,4,5,6-tetrahydro-[1,1'-biphenyl]-2-yl)methyl) piperazine (26) dihydrochloride IPA solvate[20]

To a 500 L reactor were charged with *tert*-butyl 4-((4'-chloro-5,5-dimethyl-3,4,5,6-tetrahydro-[1,1'-biphenyl]-2-yl)methyl) piperazine-1-carboxylate **29** (33.0 kg, 78.8 mol., 1.0 equiv.) and isopropyl alcohol (IPA, 258 kg). To the mixture was added 27.0 kg of 37% HCl aq. solution (274.1 mol%, 3.5 equiv.). The reaction mixture was adjusted to 65 °C and agitated for NLT 12 h until the starting material **29** was consumed monitored by HPLC. The resulting product slurry was then cooled to 0 °C at a rate of 10 °C/h, and mixed for 2 h. The product was collected by centrifugation, and washed with IPA (26 kg). The wet cake was dried at 50 °C under vacuum for 24 h to give 34.2 kg (96%) of the desired product (**26**) as a *bis*-hydrochloride IPA solvate: MS-ESI (m/z): 319.0 (M+1); ^{1}H NMR (D_2O): δ 1.00 (6H, s), 1.19 (6H, IPA, d, J = 6.0 Hz), 1.65 (2H, t, J = 6.1 Hz), 2.14 (2H, s, br), 2.26 (2H, m), 3.36 (br, 4H), 3.55 (4H, s, br), 3.82 (2H, s), 4.02(1H, IPA, septet, J = 6.0 Hz), 7.16 (2H, d, J = 8.1 Hz), 7.45 (2H, d, J = 8.1 Hz).

Synthesis of *tert*-butyl 2-((1H-pyrrolo[2,3-b]pyridin-5-yl)oxy)-4-(4-((4'-chloro-5,5-dimethyl-3,4,5,6-tetrahydro-[1, 1'-biphenyl]-2-yl)methyl)piperazin-1-yl)benzoate (23c) [20]

General considerations: this chemistry is considered air and moisture sensitive. While the catalyst precursors in their solid, dry form can be handled and stored in air without special precautions, contact with even small amounts of solvent may render them susceptible to decomposition. As a result, traces of oxygen or other competent oxidants (e.g., solvent peroxides) must be removed prior to combination of the catalyst precursors with solvent and care must be used to prevent ingress of oxygen during the reaction. Also, care must be taken to use dry equipment, solvents, and reagents to prevent formation of undesirable byproducts. The

NaO*t*Bu used in this reaction is hygroscopic and it should be properly handled and stored prior to or during use.

Freebase Solution of 26 in toluene: To a 250 L reactor were charged with l-((4'-chloro-5,5-dimethyl-3,4,5,6-tetrahydro-[1,1'-biphenyl]-2-yl)methyl) piperazine dihydrochloride IPA solvate **26** (13.4 kg, 29.7 mol, 1.0 equiv.), toluene (99 kg), and 20% K_3PO_4 aq. solution (107 kg). The resulting biphasic mixture was stirred at 25 °C for 30 min. The layers were separated and the upper organic layer was washed with 25% NaCl aq. solution (54 kg). The organic layer was concentrated to give 55 L. The solution was filtered to remove the inorganic salts, and the solids were rinsed with toluene (10 kg). The combined filtrate was further concentrated under vacuum to 40 L of the freebase solution of **26** in toluene. This solution was used in the coupling reaction without further purification. A small amount of reference sample **26** of the freebase was obtained by removing solvent under vacuum to give off-white solid: mp: 71.9 °C; MS-ESI (m/z): 319.0 (M+1); ^{1}H NMR (CD_3Cl): δ 0.89 (6H, s), 1.37 (2H, t, J = 6.5 Hz), 1.47 (1H, s, br), 1.91 (2H, s, br), 2.10 (6H, m), 2.67 (2H, s), 2.73 (4H, t, J = 4.8 Hz), 6.88 (2H, d, J = 8.1 Hz), 7.17 (2H, d, J = 8.1 Hz).

Coupling Reaction: To a 250 L reactor were charged with NaO*t*-Bu (18.5 kg, 192.5 mol, 6.5 equiv.) and anhydrous THF (68 kg). The resulting mixture was stirred at 20 °C for 30 min, filtered and rinsed with THF (8 kg). The filtered NaO*t*-Bu solution was diluted with the free base solution of **26** prepared above. This resulting solution was evacuated and purged with N_2 for several times until oxygen level is NMT 40 ppm monitored by an oxygen monitor and held under N_2. To a separate 500 L reactor were charged with *tert*-butyl 2-((1H-pyrrolo[2,3-b]pyridin-5-yl)oxy)-4-bromobenzoate **4c** (12.0 kg, 30.8 mol, 1.04 equiv.), $Pd_2(dba)_3$ (220 g, 0.24 mol, 1.6 mol% of Pd loading), and Amphos ligand (128 g, 0.48 mol., 1.6 mol%). The 500 L reactor was

carefully evacuated and purged with N_2 until oxygen level is NMT 40 ppm monitored by an oxygen monitor. Using N_2 pressure, the above inerted solution of the freebase of **26** and NaO*t*-Bu in toluene / THF was transferred into the 500 L reactor containing catalyst, ligand, and **4c**. The resulting mixture was heated to 55 °C and stirred for NLT 8 h until the starting material **26** was consumed monitored by HPLC. After the reaction completion, the reaction mixture was cooled to 20 °C and was diluted with THF (68 kg) and 12% NaCl aq. solution (95 kg). The mixture was stirred at 20 °C for 30 min, and the layers were separated. The organic layer was washed twice with a freshly prepared solution of a mixture of 5% *L*-cysteineand5% $NaHCO_3$ aq. solution (95 kg) and then 12% NaCl aq. solution (95 kg). The product solution was concentrated under vacuum to 100 L. The mixture was filtered, and rinsed with THF (10 kg). The combined filtrate was concentrated under vacuum to 55 L, and chased three times with toluene (55 kg) to 55 L. The crude product solution was reheated to 90 °C and held for 15 min to achieve completed dissolution. The temperature of the solution was then adjusted to 75 °C. To the solution was slowly added cyclohexane (184 kg) while maintaining the internal temperature at 75°C, this is then followed by addition of the seed material (160 g, 1%). The mixture was cooled to 65 °C and stirred for NLT 1 h. The resulting slurry was cooled to 25 °C in 8 h and then held at 25 °C for 4 h. The solids were centrifuged and washed with cyclohexane (22 kg). The wet-cake was dried at 60 °C under vacuum to give 16.5 kg (89% yield) of the desired product **23c** as a white solid: mp: 155.4 °C; MS-ESI (m/z): 627.3 (M+1); ^{1}H NMR (DMSO-d_6): δ 0.93 (6H, s), 1.27 (9H, s), 1.38 (2H, t, J = 6.4 Hz), 1.94 (2H, s), 2.08-2.28 (6H, m), 2.74 (2H, s), 3.02-3.19 (4H, m), 6.33 (1H, dd, J = 3.4, 1.9 Hz), 6.38 (1H, d, J = 2.4 Hz), 6.72 (1H, dd, J = 9.0, 2.4 Hz), 6.99-7.06 (2H, m), 7.29 (1H, d, J = 2.7 Hz), 7.30-7.36 (2H, m), 7.41-7.44 (1H, m), 7.64 (1H, t, J = 6.7 Hz), 7.94 (1H, d, J = 2.7 Hz), 11.53 (1H, s).

Synthesis of 2-((1H-pyrrolo[2,3-b]pyridin-5-yl)oxy)-4-(4-((4'-chloro-5,5-dimethyl-3,4,5,6-tetrahydro-[1,1'-biphenyl] -2-yl)methyl)piperazin-1-yl)benzoic acid (2) [20]

To a 500 L reactor were charged with *tert*-butyl 2-((1H-pyrrolo[2,3-b]pyridin-5-yl)oxy)-4-(4-((4'-chloro-5,5-dimethyl-3,4,5,6-tetrahydro-[1,1'-biphenyl]-2-yl)methyl)piperazin-1-yl)benzoate **23c** (12.7 kg, 20.2 mol, 1.0 equiv.) and 2-MeTHF (75 kg). To this mixture was charged a solution of KO*t*-Bu (13.6 kg, 121.2 mol, 6.0 equiv.) in 2-MeTHF (89 kg) and H_2O (1.5 kg, 83.2 mol., 4.1 equiv.). The reaction mixture was heated to 50 °C and mixed for 2 h until the starting material **23c** was consumed monitored by HPLC. After the reaction completion, the reaction solution was cooled to 20 °C and was washed twice with the 14% KH_2PO_4 aq. solution (114 kg) followed by water (114 kg). The organic product layer was filtered and the filter was rinsed with 2-MeTHF (10 kg). The combined filtrate was concentrated under vacuum to 65 L and heated to 70 °C to dissolve all solids. Heptane (44 kg) was added slowly at 70 °C. The resulting slurry was stirred for 1 h., cooled slowly to 20 °C and held for 2 h. Solids were then collected by centrifugation, and the filter cake was washed with 2:1 (v/v) mix of heptane/2-MeTHF (19 Kg). The solid was dried under vacuum at 80 °C overnight to afford 10.1 Kg (88% yield) of the desired product **2** as an off-white solid: mp: 208.6 °C. MS-ESI (m/z): 571.2 (M+1); ^{1}H NMR (DMSO-d_6): δ 0.91 (6H, s), 1.37 (2H, t, J = 6.4 Hz),1.94 (2H, s, br), 2.15 (6H, m), 2.71 (^{2}H, s, br), 3.09 (4H, m), 6.31 (1H, d, J = 2.3 Hz), 6.34 (1H, dd, J = 3.4, 1.9 Hz), 6.7 (1H, dd, J = 9.0,2.4 Hz), 7.02 (2H, m), 7.32 (2H, m), 7.37 (1H, d, J = 2.6 Hz), 7.44 (1H, t, J = 3.0 Hz), 7.72 (1H, d, J = 9.0 Hz), 7.96 (1H, d, J = 2.7 Hz) & 11.59 (1H, m).

Synthesis of 3-nitro-4-(((tetrahydro-2H-pyran-4-yl) methyl)amino)-benzenesulfonamide (**3**)

To a 200 L reactor were charged 4-chloro-3-nitrobenzenesulfonamide **24b** (6.0 kg, 25.4 mol, 1.0 equiv.), acetonitrile (71 kg), diisopropylethylamine (10.5 kg, 81.4 mol, 3.2 equiv.), and (tetrahydro-2*H*-pyran-4-yl)methanamine **25** (4.2 kg, 36.5 mol, 1.4 equiv.). The temperature of the reaction mixture was adjusted to 80 °C and the mixture was agitated for NLT 24 h until the starting material **24b** was consumed monitored by HPLC. After the reaction completion, the product solution was cooled down to 40 °C and agitated for 1 h until precipitation observed. The product slurry was further cooled to 20 °C. Water (45 kg) was slowly added over 1 h at 20 °C, the resulting mixture was cooled to 10 °C and agitated for NLT 2 h. The solid was collected by centrifugation. The wet cake was washed with 1:1 (v/v) mix of CH_3CN:H_2O (21 kg) and charged back to the reactor. To the reactor was then charged with H_2O (48 kg) and the product slurry was heated to 40 °C and mixed for NLT 1 h. The solids were collected by filtration. The wet cake was rinsed with water (12 kg), and dried at 75 °C under vacuum for NLT 24 h to give 7.0 kg (88% yield) of the desired product **3** as a yellow solid: mp: 191.0 °C (uncorrected); MS-ESI (m/z): 316.1 (M+1); ^{1}H NMR (DMSO-d_6): δ 1.25 (2H, m), 1.60 (2H, m), 1.89 (1H, m), 3.25 (2H, m), 3.33 (2H, m), 3.83 (2H, m), 7.27 (1H, d, J = 9.3 Hz), 7.32 (2H, NH2, s), 7.81 (1H, dd, J = 9.1, 2.3 Hz), 8.45 (1H, d, J = 2.2 Hz), 8.54 (1H, NH, t, J = 5.9 Hz).

Synthesis of 4-(4-{[2-(4-chlorophenyl)-4,4-dimethylcyclohex-1-en-1-yl]methyl}piperazin-1-yl)-N-({3-nitro-4-[(tetrahydro-2H-pyran-4-ylmethyl)amino]phenyl}sulfonyl)-2-(lH-pyrrolo[2,3-b]pyridin-5-yloxy)benzamide (1) [20]

To a 200 L reactor were charged with 3-Nitro-4-(((tetrahydro-2*H*-pyran-4-yl) methyl)amino)-benzenesulfonamide **3** (3.6 kg, 11.4 mol, 1.0 equiv.), DMAP (1.4 kg, 11.4 mol, 1.0 equiv.), *N*-ethyl-*N*′-(3-dimethylaminopropyl) carbodiimide hydrochloride **(**EDAC) (2.8 kg, 14.7 mol, 1.3 equiv.) and CH_2Cl_2 (87 kg). The mixture was agitated at 25 °C. To this mixture was charged

slowly a solution of 2-((1*H*-pyrrolo[2,3-b]pyridin-5-yl)oxy)-4-(4-((4'-chloro-5,5-dimethyl-3,4,5,6-tetrahydro-[1,1'-biphenyl] -2-yl)methyl)piperazin-1-yl)benzoic acid **2** (6.5 kg, 11.4 mol, 1.0 equiv.) and Et_3N (2.3 kg, 22.8 mol, 2.0 equiv.) in CH_2Cl_2 (60 kg) maintaining the internal temperature at 25 °C. The resulting reaction mixture was agitated at 25 °C for NLT 12 h until the starting material **2** was consumed monitored by HPLC. After the reaction completion, *N*,*N*-dimethylethylediamine (2.5 kg, 28.5 mol, 2.5 equiv.) was then charged to the mixture to quench the reaction. The quenched reaction mixture was heated to 35 °C and washed twice with 10 wt. % AcOH solution (52 kg). The lower organic product layer was diluted with more CH_2Cl_2 and MeOH (3 kg) and washed with 5% $NaHCO_3$ aq. solution (61 kg), and then with 5 % NaCl aq. solution (61 kg) at 35 °C. The lower organic product layer was separated and concentrated to ~ 84 L and diluted with MeOH (6 kg). The mixture was warmed to 38 °C, to this mixture was added EtOAc (58 kg) slowly maintaining the internal temperature at 38 °C. The resulting suspension was slowly cooled to 10 °C and filtered. The wet cake was washed twice with a 1:1 (v/v) mix of CH_2Cl_2 / EtOAc (20 kg). After drying the wet cake at 90 °C, 8.5 kg (86%) of compound **1** was isolated as a yellow solid: mp: 123.2 °C; MS-ESI (m/z): 869.4 (M+1); ^{1}H NMR (DMSO-d_6): δ 0.90 (6H, s), 1.24 (2H, m), 1.36 (2H, t, *J* = 6.4 Hz), 1.60 (2H, m), 1.87 (1H, m), 1.93 (2H, br, s), 2.12 (2H, m), 2.19 (4H, m), 2.74 (2H, br, s), 3.06 (4H, m), 3.26 (4H, m), 3.83 (2H, m), 6.17 (1H, d, *J* = 2.1 Hz), 6.37 (1H, dd, *J* = 3.4,1.9 Hz), 6.66 (1H, dd, *J* = 9.1, 2.2 Hz), 7.01 (2H, m), 7.11 (1H, d, *J* = 9.3 Hz), 7.31 (2H, m), 7.48 (3H, m), 7.78 (1H, dd, *J* = 9.3, 2.3 Hz), 8.02 (1H, d, *J* = 2.61 Hz), 8.54 (1H, d, *J* = 2.33 Hz), 8.58 (1H, NH, t, *J* = 5.9 Hz), 11.35 (1H, s), 11.65 (1H, m).

ASSOCIATED CONTENT

THE SUPPORTING INFORMATION IS AVAILABLE FREE OF CHARGE VIA THE INTERNET AT HTTP://PUBS.ACS.ORG.

^{1}H NMR,^{13}C NMR and MS spectra of compounds 32c, 4c, 12, 5, 29, 26, 26FB, 23c, 2, 3, 1, 38, 39, 40, 41

AUTHOR INFORMATION

Corresponding Author

E-mail: yiyin.ku@abbvie.com

Acknowledgement:

All authors are employees or former employee of AbbVie. The design, study conduct, and financial support for this research was provided by AbbVie. AbbVie participated in the interpretation of data, review, and approval of the publication.

6. REFERENCES

(1) The Official Venclexta Website. https://www.venclexta.com (accessed Oct 2018).

(2) (a) Mullard, A. Pioneering Apoptosis-targeted Cancer Drug Poised for FDA Approval. *Nat. Rev. Drug Discovery* **2016**, *15*, 147—149. (b) Delbridge, A. R. D.; Grabow, S.; Strasser, A.; Vaux, D. L. Thirty Years of BCL-2: Translating Cell Death into Novel Cancer Therapies. *Nat. Rev. Cancer* **2016**, *16*, 99—109.

(3) Leverson J. D.; Phillips D. C.; Mitten M. J.; Boghaert E. R.; Diaz D.; Tahir S. K.; Belmont, L. D.; Nimmer, P.; Yu Xiao, Y.; Ma, X. M.; Lowes, K. N.; Kovar, P.; Chen, J.; Jin, S.; Smith, M.; Xue, J.; Zhang, H.; Oleksijew, A.; Magoc, T. J.; Vaidya, K. S.; Albert, D. H.; Tarrant, J. M.; La, N.; Wang, L.; Tao, Z.; Wendt, M. D.; Sampath, D.; Rosenberg, S. H.; Tse, C.; Huang, D. C. S.; Fairbrother, W. J.; Elmore, S. J.; Souers, A. J. Exploiting Selective BCL-2 Family Inhibitors

to Dissect Cell Survival Dependencies and Define Improved Strategies for Cancer Therapy. *Sci Trasl. Med.* **2015**, *7*, 1—11.

(4) Souers, A. J.; Leverson, J. D.; Boghaert, E. R.; Ackler, S. L.; Catron, N. D.; Chen, J.; Dayton, B. D.; Ding, H.; Enschede, S. H.; Fairbrother, W. J.; Huang, D. C. S.; Hymowitz, S. G.; Jin, S.; Khaw, S. L.; Kovar, P. J.; Lam, L. T.; Lee, J.; Maecker, H. L.; Marsh, K. C.; Mason, K. D.; Mitten, M. J.; Nimmer, P. M.; Oleksijew, A.; Park, C. H.; Park, C.; Phillips, D. C.; Roberts, A. W.; Sampath, D.; Seymour, J. F.; Smith, M. L.; Sullivan, G. M.; Tahir, S. K.; Tse, C.; Wendt, M. D.; Xiao, Y.; Xue, J. C.; Zhang, H.; Humerickhouse, R. A.; Rosenberg, S. H.; Elmore, S. W. ABT-199, A Potent and Selective BCL-2 Inhibitor, Achieves Antitumor Activity While Sparing Platelets. *Nat. Med. (New York, NY, U.S.)* **2013**, *19*, 202—208.

(5) Cory, S.; Huang, D. C.; Adams, J. M. The Bcl-2 Family: Roles in Cell Survival and Oncogenesis. *Oncogene* **2003**, *22*, 8590—8607.

(6) Reed, J. C. Bcl-2-Family Proteins and Hematologic Malignancies: History and Future Prospects. *Blood* **2008**, *111* (7), 3322—3330.

(7) Adams, J. M.; Cory, S. The Bcl-2 Apoptotic Switch in Cancer Development and Therapy. *Oncogene* **2007**, *26*, 1324—1337

(8) Strasser, A.; Cory, S.; Adams, J. M. Deciphering the Rules of Programmed Cell Death to Improve Therapy of Cancer and Other Diseases. *EMBO J.* **2011**, *30*, 3667—3683.

(9) Hanahan, D.; Weinberg, R. A. The Hallmarks of Cancer. *Cell (Cambridge, MA, U.S.)* **2000**, *100*, 57—70.

(10) Czabotar, P. E.; Lessene, G.; Strasser, A.; Adams, J. M. Control of Apoptotsis by the BCL-2 Protein Family: Implications for Physiology and Therapy. *Nat. Rev. Mol. Cell Biol.* **2014,** *15*, 49—63.

(11) Delbridge, A. R.; Strasser, A. The BCL-2 Protein Family: BH3-mimetics and Cancer Therapy. *Cell Death Differ.* **2015**, *22*, 1071—1080.

(12) Shamas-Din, A.; Kale, J.; Leber, B.; Andrews, D. W. Mechanism of Action of Bcl-2 Family Proteins. *Cold Spring Harb*. *Perspect. Biol.* **2013**, *5*, a008714.

(13) Moldoveanu, T.; Follis, A. V.; Kriwacki, R. W.; Green, D. R. Many Players in BCL-2 Family Affairs. *Trends Biochem. Sci.* **2014**, *39*, 101—111.

(14) Del Gaizo Moore, V.; Brown, J. R.; Certo, M.; Love, T. M.; Novina, C. D.; Letai, A. Chronic Lymophocytic Leukemia Requires BCL-2 to Sequester Prodeath BIM. Explaining Sensitivity to BCL-2 Antagonist ABT-737. *J. Clin. Invest.* **2007**, *117*, 112—121.

(15) Deng, J.; Carlson, N.; Kunihiko, T.; Dal Cin, P.; Shipp, M.; Letai, A. BH3 Profiling Identifies Three Distinct Classes of Apoptotic Blocks to Predict Response to ABT-737 and Conventional Chemotherapeutic Agents. *Cancer Cell* **2007**, *12*, 171—185.

(16) Tse, C.; Shoemaker, A. R.; Adickes, J.; Anderson, M. G.; Chen, J.; Jin, S.; Johnson, E. F.; Marsh, K. C.; Mitten, M. J.; Nimmer, P.; Roberts, L.; Tahir, S. K.; Xiao, Y.; Yang, X.; Zhang, H.; Fesik, S.; Rosenburg, S. H.; Elmore, S. W. ABT-263: A Potent and Orally Bioavailable Bcl-2 Family Inhibitor. *Cancer Res.* **2008**, *68*, 3421—3428.

(17) Wilson, W. H.; O'Connor, O. A.; Czuczman, M. S.; LaCasce, A. S.; Gerecitano, J. F.; Leonard, J. P.; Tulpule, A.; Dunleavy, K.; Xiong, H.; Chui, Y.; Cui, Y.; Busman, T.; Elmore, S.

W.; Rosenburg, S. H.; Krivoshik, A. P.; Enschede, S. H.; Humerickhouse, R. A. Navitoclax, A Targeted High-affinity Inhibitor of BCL-2, in Lymphoid Malignancies: A Phase 1 Dose-escalation Study of Safety, Pharmacokinetics, Pharmacodynamics, and Antitumor Activity. *Lancet Oncol.* **2010**, *11*, 1149—1159.

(18) (a) Smietana, K.; Siatkowski, M.; Møller, M. Trends in Clinical Success Rates. *Nat. Rev. Drug Discov.* **2016**, *15*, 379—380. (b) Mullard, A. Parsing Clinical Success Rates. *Nat. Rev. Drug Discov.* **2016**, *15*, 447. (c) Carter, P. H.; Berndt, E. R.; DiMasi, J. A.; Trusheim, M. Investigating Investment in Biopharmaceutical R&D. *Nat. Rev. Drug Discov.* **2016, *15*,** 673—674.

(19) Bruncko, M.; Ding, H.; Doherty, G. A.; Elmore, S. W.; Hansen, T. M.; Hasvold, L.; Hexamer, L.; Kunzer, A. R.; Mantei, R. A.; McClellan, W. J.; Park, C. H.; Park, C.; Petros, A. M.; Song, X.; Souers, A. J.; Sullivan, G. M.; Tao, Z.; Wang, G. T.; Wang, L.; Wang, X.; Wendt, M. D. BCL-2-Selective Apoptosis-inducing Agents for the Treatment of Cancer and Immune Diseases, U.S. Pat. Appl. Publ. US 20100298321 A1, Nov 25, 2010.

(20) Chan, V. S.; Christesen, A. C.; Grieme, T. A.; Ku, Y.; Mulhern, M. M.; Pu, Y. M. Processes for the Preparation of an Apoptosis-Inducing Agent, U.S. Pat. Appl. Publ. US 20140275540 A1, Sep 18, 2014.

(21) (a) Miyaura, N.; Yamada, K; Suzuki, A. A New Stereospecific Cross-coupling by the Palladium-catalyzed Reaction of 1-Alkenylboranes with 1-Alkenyl or 1-Alkynyl Halides. *Tetrahedron Lett.* **1979**, *20*, 3437—3440. (b) Miyaura, N.; Suzuki, A. Stereoselective Synthesis of Arylated (*E*)-Alkenes by the Reaction of Alk-1-enylboranes with Aryl Halides in the Presence of Palladium Catalyst. *J. Chem. Soc. Chem. Comm.* **1979**, *19*, 866—867. (c) Miyaura, N.;

Suzuki, A. Palladium-catalyzed Cross-coupling Reactions of Organoboron Compounds. *Chemical Reviews* **1995**, *95*, 2457—2483. (d) Suzuki, A. Synthetic Studies Via the Cross-coupling Reaction of Organoboron Derivatives with Oragnic Halides. *Pure Appl. Chem*. **1991**, *63*, 419—422. (e) Suzuki, A. Recent Advances in the Cross-coupling Reactions of Organoboron Derivatives with Organic Electrophiles. *J. Organomet. Chem.* **1999**, *576*, 147—168.

(22) (a) Teasdale, A.; Elder, D.; Chang, S.-J.; Wang, S.; Thompson, R.; Benz, N.; Flores, I. H. S. Risk Assessment of Genotoxic Impurities in New Chemical Entities: Strategies to Demonstrate Control. *Org. Process Res. Dev.* **2013**, *17*, 221—230. (b) Teasdale, A.; Fenner, S.; Ray, A.; Ford, A.; Phillips, A. A Tool for the Semiquantitative Assessment of Potentially Genotoxic Impurity (PGI) Carryover into API Using Physicochemical Parameters and Process Conditions. *Org. Process Res. Dev.* **2010**, *14*, 943—945.

(23) Doherty, G. A.; Elmore, S. W.; Hansen, T. M.; Hasvold, L. A.; Mantei, R.; Souers, A. J.; Tao, Z.; Wang, G. T.; Wang, L. Apoptosis-Inducing Agents for the Treatment of Cancer and Immune and Autoimmune Diseases, U.S. Pat. Appl. Publ. US 20110124628 A1, May 26, 2011.

(24) Doherty, G. A.; Hansen, T. M.; Hexamer, L. A.; Mantei, R. A.; Sullivan, G. M.; Tao, Z.; Wang, G. T.; Wang, L.; Wang, X. Apoptosis-Inducing Agents for the Treatment of Cancer and Immune and Autoimmune Diseases, U.S. Pat. Appl. Publ. US 20100298323 A1, Nov 25, 2010.

(25) Catron, N. D.; Lindley, D. J.; Miller, J.; Schmitt, E. A.; Tong, P. Solid Dispersions Containing an Apoptosis-Inducing Agent, PCT Int. Appl. WO 2012058392 A1, May 03, 2012.

(26) Catron, N. D.; Chen, S.; Gong, Y.; Zhang, G. G. Salts and Crystalline Forms of an Apoptosis-Inducing Agent, PCT Int. Appl. WO 2012071336 A1, May 31, 2012.

(27) ICH Q1A (R2) Stability Testing of New Drug Substances and Products. http://www.ich.org/fileadmin/Public_Web_Site/ICH_Products/Guidelines/Quality/Q1A_R2/Step4/Q1A_R2__Guideline.pdf (accessed Oct 2018).

(28) (a) Sperotto, E.; van Klink, G. P. M.; de Vries, J. G.; van Koten, G. Aminoarenethiolato-copper(I) as (pre-)Catalyst for the Synthesis of Diaryl Ethers from Aryl Bromides and Sequential C-O/C-S and C-N/C-S Cross Coupling Reactions. *Tetrahedron* **2010**, *66*, 9009—9020. (b) Benyahya, S.; Monnier, F.; Taillefer, M.; Man, M. W. C.; Bied, C.; Ouazzani, F. Efficient and Versatile Sol-Gel Immobilized Copper Catalyst for Ullmann Arylation of Phenols. *Adv. Synth. Catal.* **2008**, *350*, 2205—2208. (c) Liu, X.; Zhang, S. Efficient Iron/Copper-Cocatalyzed O-Arylation of Phenols with Bromoarenes. *Synlett* **2011**, *2*, 268—272. (d) Mulla, S. A. R.; Inamdar, S. M.; Pathan, M. Y.; Chavan, S. S. Ligand Free, Highly Efficient Synthesis of Diaryl Ether over Copper Fluorapatite as Heterogeneous Reusable Catalyst. *Tetrahedron Lett.* **2012**, *53*, 1826—1829. (e) Verma, S.; Kumar, N.; Jain, S. L. Copper(II) *trans*-Bis-(glycinato): An Efficient Heterogeneous Catalyst for Cross Coupling of Phenols with Aryl Halides. *Tetrahedron Lett.* **2012**, *53*, 4665—4668.

(29) (a) Tsvelikhovsky, D.; Buchwald, S. L. Concise Palladium-catalyzed Synthesis of Dibenzodiazepines and Structural Analogues. *J. Am. Chem. Soc.* **2011**, *133*, 14228—14231. (b) Ruiz-Castillo, P.; Buchwald, S. L. *Chem. Rev.* **2016**, *116*, 12564—12649. (c) Stambuli, J. P.; Kuwano, R.; Hartwig, J. F. Unparalleled Rates for the Activation of Aryl Chlorides and Bromides: Coupling with Amines and Boronic Acids in Minutes at Room Temperature. *Angew Chem. Int. Ed.* **2002**, *41*, 4746—4748. (d) Seechurn, C. C. C. J.; Sperger, T.; Scrase, T. G.; Schoenebeck, F.; Colacot, T. J. Understanding the Unusual Reduction Mechanism of Pd(II) to Pd(I): Uncovering Hidden Species and Implications in Catalytic Cross-coupling Reactions. *J.*

Am. Chem. Soc. **2017**, *139*, 5194—5200. (e) Henderson, J. L.; McDermott, S. M.; Buchwald, S. L. Palladium-catalyzed Amination of Unprotected Halo-7-azaindoles. *Org. Lett*. **2010**, *12*, 4438—4441. (f) Henderson, J. L.; Buchwald, S. L. Efficient Pd-catalyzed Amination Reactions for Heterocycle Functionalization. *Org. Lett.* **2010**, *12*, 4442—4445. (g) Guram, A. S.; King, A. O.; Allen, J. G.; Wang, X.; Schenkel, L. B.; Chan, J.; Bunel, E. E.; Faul, M. M.; Larsen, R. D.; Martinelli, M. J.; Reider, P. J. New Air-stable Catalysts for General and Efficient Suzuki-Miyuara Cross-coupling Reactions of Heteroaryl Chlorides. *Org. Lett*. **2006**, *8*, 1787—1789.

(30) (a) Paul, F.; Patt, J.; Hartwig, J. F. Palladium-catalyzed Formation of Carbon-Nitrogen Bonds. Reaction Intermediates and Catalyst Improvements in the Hetero Cross-coupling of Aryl Halides and Tin Amides. *J. Am. Chem. Soc.* **1994**, *116*, 5969—5970. (b) Guram, A. S.; Buchwald, S. L. Palladium-catalyzed Aromatic Aminations with *In Situ* Generated Aminostannanes. *J. Am. Chem. Soc.* **1994**, *116*, 7901—7902. (c) Louie, J.; Hartwig, J. F. Palladium-catalyzed Synthesis of Arylamines from Aryl Halides. Mechanistic Studies Lead to Coupling in the Absence of Tin Reagents. *Tetrahedron Lett.* **1995**, *36*, 3609—3612. (d) Guram, A. S.; Rennels, R. A.; Buchwald, S. L. A Simple Catalytic Method for the Conversion of Aryl Bromides to Arylamines. *Angew. Chem. Int. Ed.* ***1995***, *34*, 1348—1350. (e) Driver, M. S.; Hartwig, J. F. Carbon-Nitrogen Bond-forming Reductive Elimination of Arylamines from Palladium(II) Phosphine Complexes. *J. Am. Chem. Soc.* **1997**, *119*, 8232—8245. (f) Hartwig, J. F.; Richards, S.; Barañano, D.; Paul, F. Influences on the Relative Rates for C-N Bond-forming Reductive Elimination and β–Hydrogen Elimination of Amides. A Case Study on the Origins of Competing Reduction in the Palladium-catalyzed Amination of Aryl Halides. *J. Am. Chem. Soc.* **1996**, *118*, 3626—3633.

(31) Sunesson, Y.; Limé, E.; Nilsson Lill, S. O.; Meadows, R. E.; Norrby, P.-O. Role of the Base in Buchwald–Hartwig Amination, *J. Org. Chem.* **2014**, *79*, 11961-11969.

(32) Gassman, P. G.; Schenk, W. N. A General Procedure for the Base-promoted Hydrolysis of Hindered Esters at Ambient Temperatures. *J. Org. Chem.* **1977**, *42*, 918—920.

(33) Q11 Development And Manufacture of Drug Substances. Section V. www.fda.gov/downloads/drugs/guidances/ucm261078.pdf (accessed Oct 2018).